Detectors in Particle Physics

1. Interactions of particles and radiation with matter (brief recap)
2. Tracking detectors, vertexing and magnetic spectrometer
3. Calorimeters
4. Particle identification
5. Detector systems

1. Interactions of particle and radiation w/ matter

Energy loss of heavy charged particles: ($m > m_e$)

Energy loss of particles from ionization of matter atoms through collisions with shell electrons.

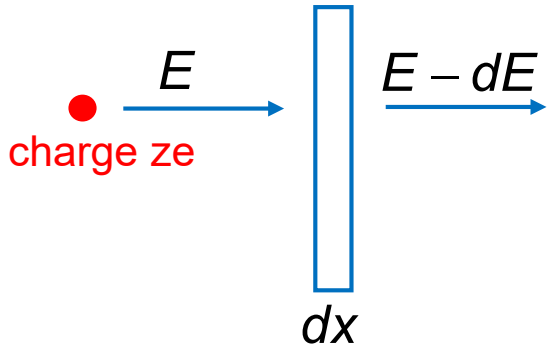

Average specific energy loss dE/dx described by Bethe-Bloch formula

$$\langle \frac{dE}{dx} \rangle_{\text{ion}} = - \underbrace{\left(\rho N_A \frac{Z}{A} \right)}_{n_e} 4\pi r_e^2 m_e c^2 z^2 \cdot \frac{1}{\beta^2} \cdot \left(\ln \frac{2 m_e c^2 \gamma^2 \beta^2}{I} - \beta^2 \right)$$

ρ = density, n_e= e$^-$ density
N_A = Avogadro number
Z, A = charge and mass number
r_e = class. Electron radius
I = effective ionization energy

z = charge of the projectile
β = velocity of the projectile

$$r_e = \frac{e^2}{4\pi m_e c^2}$$

To reduce the material dependence one often divides the specific energy loss by the material density ρ

$$\left\langle \frac{dE}{dx} \right\rangle \rightarrow \left\langle \frac{1}{\rho}\frac{dE}{dx} \right\rangle$$

(this is often hidden by redefining the ρx → x'

$$\frac{1}{\rho}\langle\frac{dE}{dx}\rangle = -\underbrace{\left(N_A 4\pi r_e^2 m_e c^2\right)}_{K} z^2 \frac{Z}{A} \cdot \frac{1}{\beta^2} \cdot \left(\ln \frac{2m_e c^2 \gamma^2 \beta^2}{I} - \beta^2\right)$$

$$K/A = 0.307\,\mathrm{MeV\,g^{-1}\,cm^2} \text{ mit } A = 1\,\mathrm{g \cdot Mol^{-1}}$$

w/ Z/A≈ 0.5 for most materials: K Z/A ≈ 0.150 MeV $g^{-1}cm^2$

Energy loss through ionization.

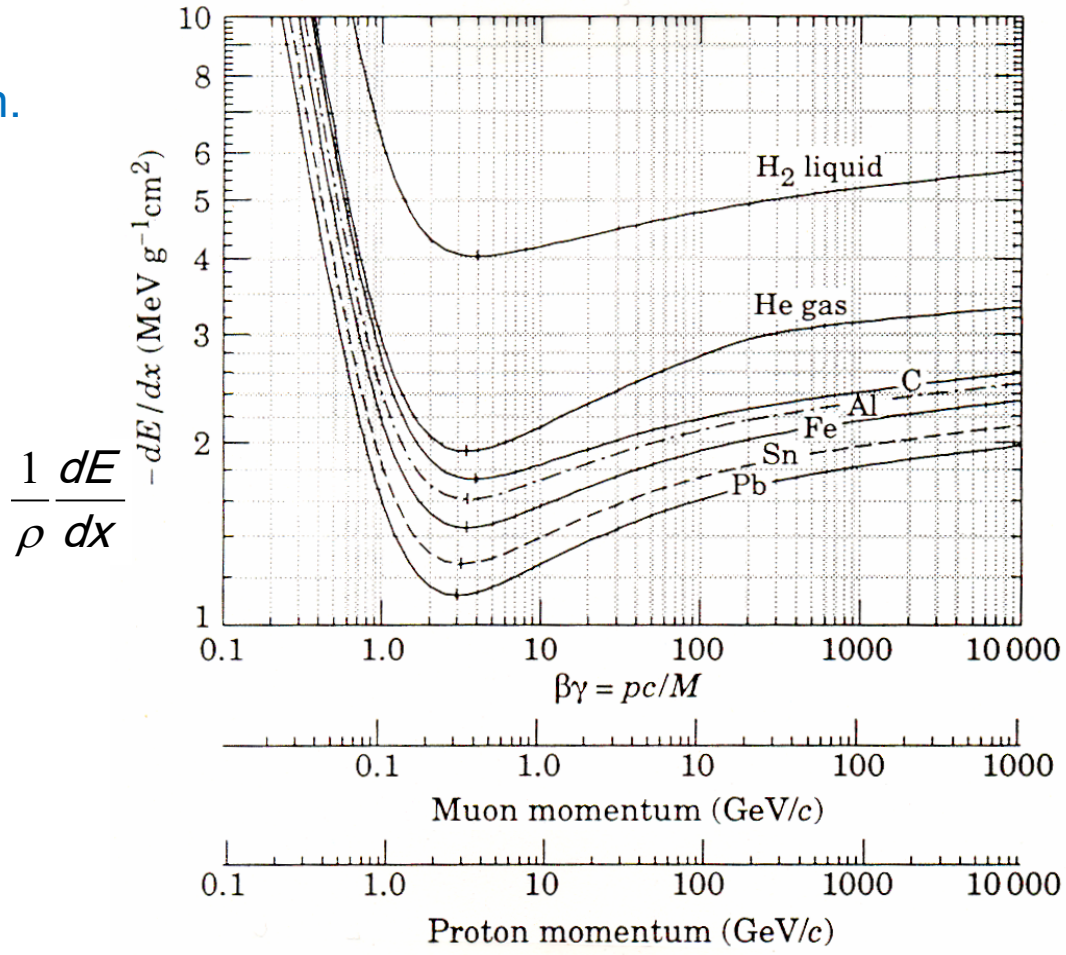

Plot from PDG

difference: Z/A

- ~$1/\beta^2$ for small $\beta\gamma$
- Minimum at $\beta\gamma$ = 3…4 w/ dE/dx =1…2 MeV g^{-1} cm^2 (multiply with ρ to get dE/dx): if one ignores Bremsstrahlung (for muons up to $\beta\gamma$ = O(1000) i.e. 100 GeV ok) particles are quasi "minimal ionizing" also above $\beta\gamma$ of 3.
- For small $\beta\gamma$, dE/dx can be used for particle ID (see below)

Multiple scattering:

Multiple collisions of the projectile with the atoms of the material (stochastic process) leads to a deflection of the particle

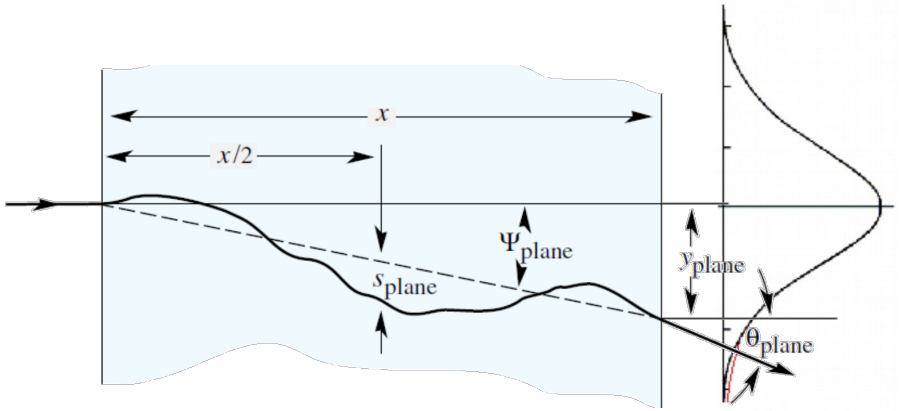

For small angles the deflection follows a Gaussian distribution, at least for the central 98%.

$$\frac{1}{\sqrt{2\pi}\,\theta_0}\exp\left(-\frac{\theta^2_{\text{plane}}}{2\theta_0^2}\right)$$

The widths of the Gaussian can be approximated. Depending if one measures the deflection in a plane or in 3D one obtains:

$$\theta_0 = \theta^{\text{rms}}_{\text{plane}} = \frac{1}{\sqrt{2}}\,\theta^{\text{rms}}_{\text{space}}$$

One finds that the width parameter θ_0 depends on the path x through the material in units of the radiation length X_0 and on the particle's momentum. It is less for high momentum particles.

$$\theta_0 = \frac{13.6\ \text{MeV}}{\beta c p}\, z\sqrt{\frac{x}{X_0}}$$

Cherenkov-radiation: (→ negligible energy loss of the particle)

When a particle traverses a medium with a velocity β (particle velocity β close to c for highly relativistic particles) which is larger than the speed of light within that medium, the particle emits Cherenkov radiation (threshold $\beta > 1/n$).

Cherenkov radiation is emitted on a cone with an opening angle θ_c

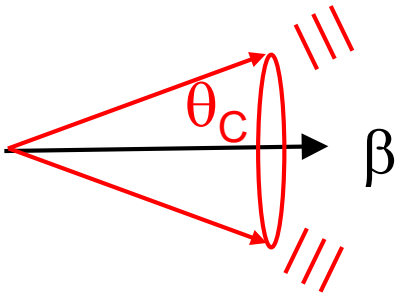

$$\cos\theta_C = \frac{1}{\beta n}$$

Emitted photons are ranging from the visible blue spectrum to the ultraviolet and The number of photons per unit length of the radiator and per wave-length unit is

$$\frac{d^2N_\gamma}{dx\,d\lambda} = \frac{2\pi\alpha z^2}{\lambda^2}\left(1 - \frac{1}{\beta^2 n(\lambda)^2}\right)$$

z is the charge of the particle.

Medium must be transparent: gases (→ Ring-Cherenkov counter) or water (e.g. large water Cherenkov detectors used for neutrino detection).

Energy loss of electrons (positrons)

For light electrons there are two competing mechanism:

- Energy loss through ionization (essentially a la Bethe-Bloch, but max. momentum transfer much larger: $\Delta E = 1/2\ E_{kin}$ Additionally there is the problem that projectile and shell electrons are undistinguishable particles)
- Energy loss through Bremsstrahlung

$$\langle \frac{dE}{dx} \rangle = \langle \frac{dE}{dx} \rangle_{\text{ion}} + \langle \frac{dE}{dx} \rangle_{\text{Brems}}$$

For high-energy electrons the energy loss by Bremsstrahlung is by far dominating. Only for very low-energy electrons the energy loss by ionization takes over.

Critical energy E_c:

$$\langle \frac{dE}{dx} \rangle_{\text{ion}} \Big|_{E_c} = \langle \frac{dE}{dx} \rangle_{\text{Brems}} \Big|_{E_c}$$

One finds empirically for solid materials: $E_c \approx 610\,\text{MeV}/(Z + 1.2)$

Remark: for lead, bremsstrahlung dominates above ~10 MeV

Bremsstrahlung:

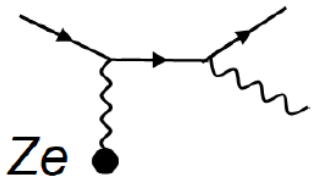

Typical length scale for Bremsstrahlung:
Radiation length X_0:

$$\frac{1}{X_0} = \rho N_A \frac{Z^2}{A} \cdot 4\alpha \cdot r_e^2 \cdot \ln\left(\frac{183}{Z^{1/3}}\right)$$

(strong Z dependence)

Energy loss:

$$\langle \frac{dE}{dx} \rangle_{\text{Brems}} = -\frac{1}{X_0} E(x)$$

Energy as function of x:

$$E(x) = E_0 e^{-\frac{x}{X_0}}$$

Energy loss of photons

Photons interact in different ways with matter. Most relevant mechanisms:

- Photo-electric effect for low energy photons
- Compton effect for photon energies between 10 keV and MeV
- Pair production for $E_\gamma > 1$ MeV ($2m_e$)

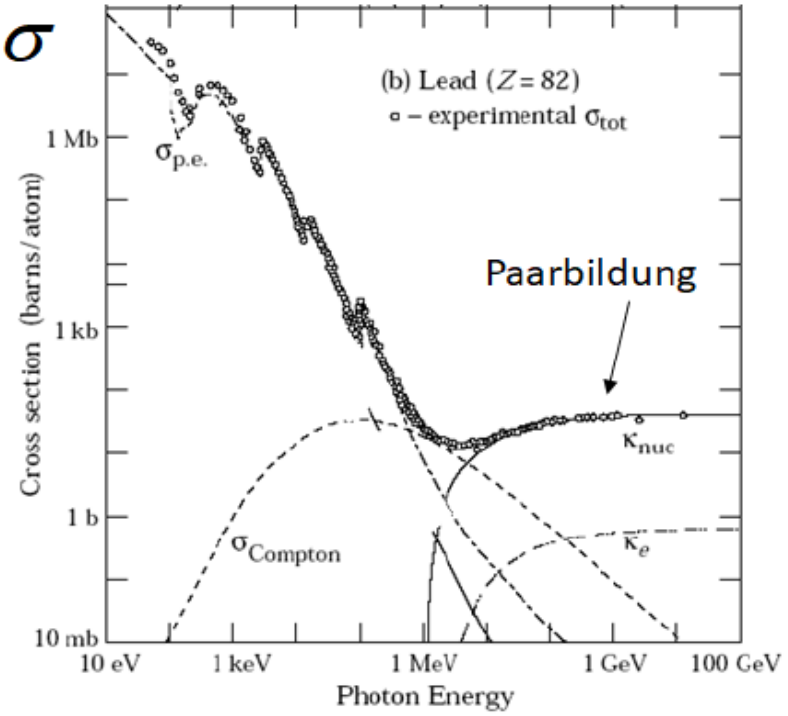

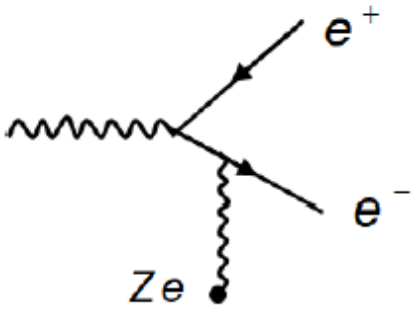

The typical length scale for pair production in matter is again the radiation length.
An exact calculation however results into 9/7 X_0 - slightly larger than for bremsstrahlung)
(both processes w/ similar Feynman diagrams)

Pair production cross section is for photon energies above 1 GeV largely constant:

$$\sigma_{\text{Paar}} = \frac{7}{9} \cdot \underbrace{\frac{A}{\rho N_A}}_{1/n} \cdot \frac{1}{X_0}$$

Electromagnetic shower

Simple shower model for higher-energy photons/electrons.
Electrons/photons make bremsstrahlung / pair production after ~X_0

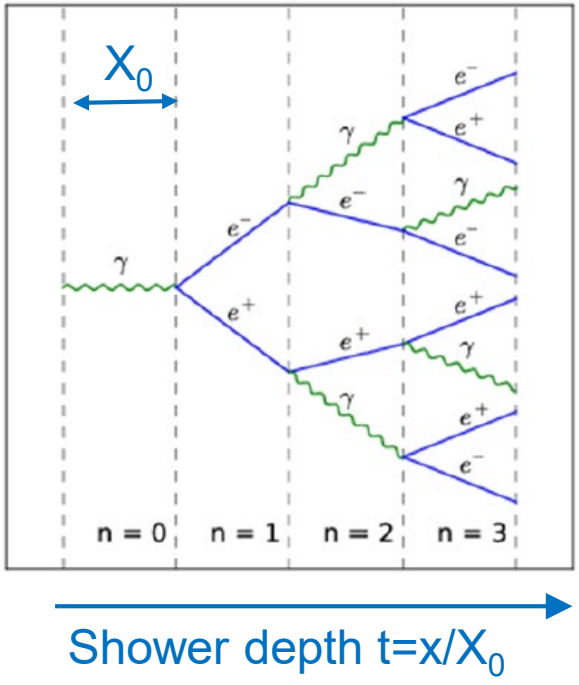

In every step the number of shower particles is doubled: $N(t) = 2^t$

The average energy of the shower particles is E/N – the shower stops when the particle energy has reached the critical energy E_C in the material:

Max. shower depth: $t_{max} = \frac{\ln(E / E_c)}{\ln 2}$

With increasing energy E of the detected particle the calorimeter depth should increase with $\sim \ln(E / E_c)$

$$E / 2^{t_{max}} = E_c$$

$$\rightarrow \ln(E / E_c) = t_{max} \ln 2 =$$

Hadronic shower

High-energy hadrons (E>>1 GeV) interact with the nuclei and the nucleons of the of the matter and produce a shower of secondary particles.

$$n, \ , p \, , \pi^{\pm} \, , K^{\pm} \, , K^{0} + A \longrightarrow$$ Shower of secondary particles

The details of the shower are more difficult to describe compared to electromagnetic showers:

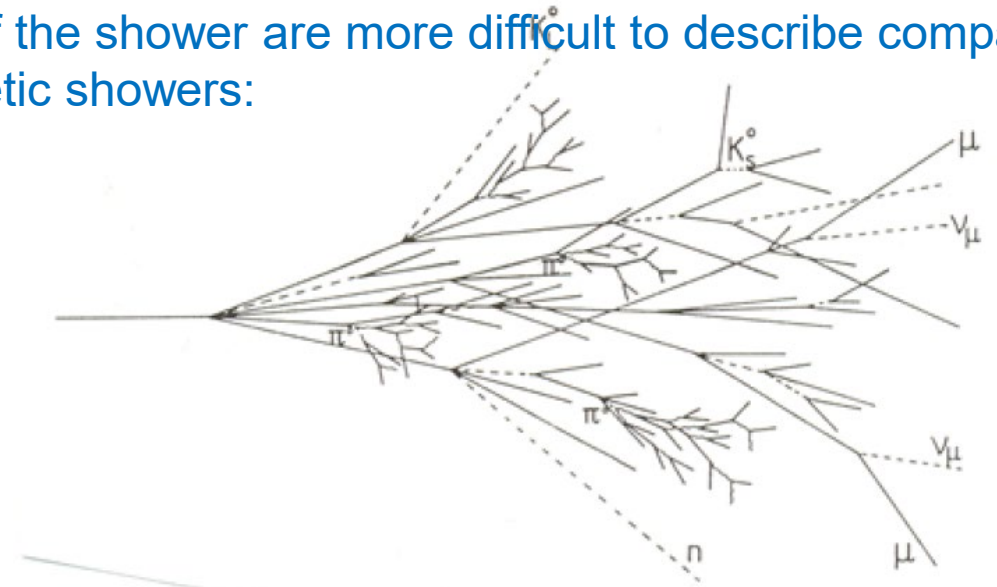

Characteristic interaction length (λ_{int}) for hadron passing matter is given by:

$$\lambda_{\text{int}} = \frac{1}{n \cdot \sigma_{\text{int}}} = \frac{A}{\rho N_A} \cdot \frac{1}{\sigma_{\text{int}}}$$

Where one finds empirically $\sigma_{\text{int}} \approx 35\,\text{mb}\, A^{0.7}$

Element	λ_{int}
Fe	16.8 cm
Pb	17.6 cm
C	39 cm

2. Tracking, vertexing and magnetic spectrometer

Reconstruct track of charged particle in an magnetic field → use the track curvature to estimate the momentum → reconstruct decay vertices.

Historical example: **Bubble chamber** (by D. Glaser in 1952, Nobel prize in 1960)

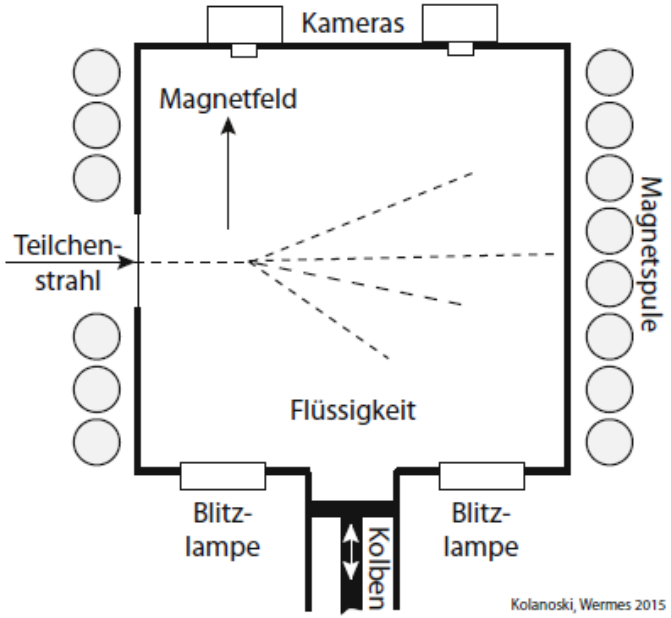

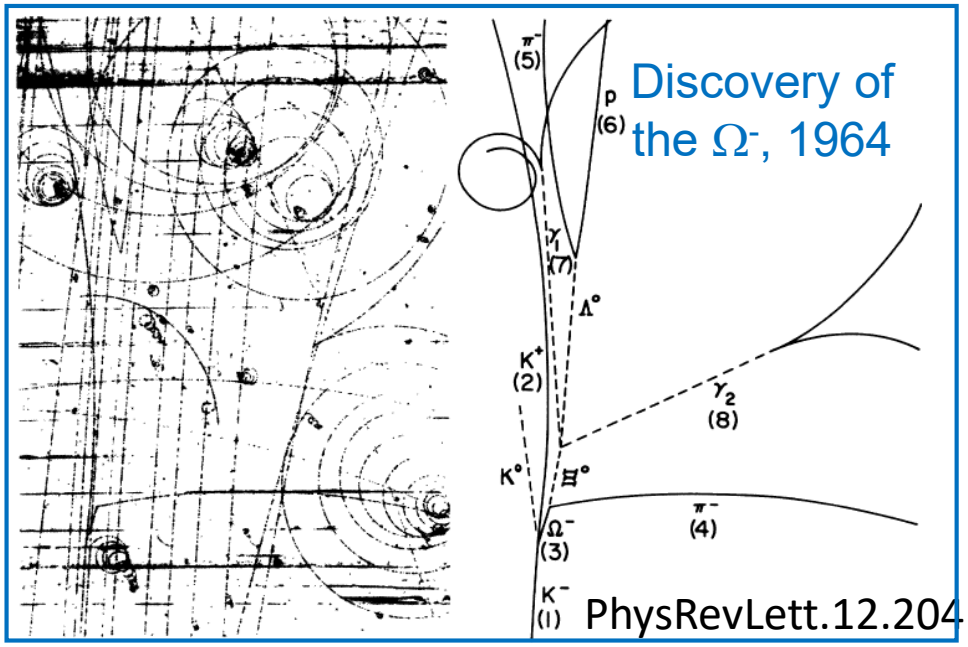

vessel filled with a super-heated transparent liquid (often H_2).

Reconstruction of tracks, decay vertices, momenta.
Disadvantage: photo w/ subsequent digitization, heavy piston to arm the detector
→ slow acquisition rate

Multi-wire proportional chambers (MWPCs)

Georges Charpak (1968), Nobel prize in 1992.

Wire chambers have revolutionized charged particle detection:
fully electronic event recording, high data acquisition rates (up to 40 MHz),
excellent position resolution when operated as drift chambers.

Detection principle:

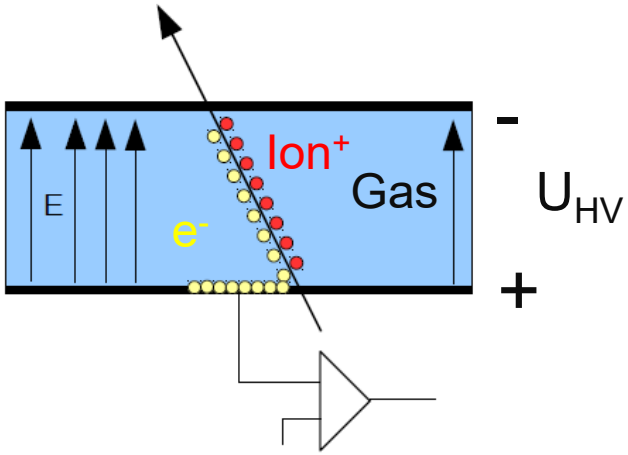

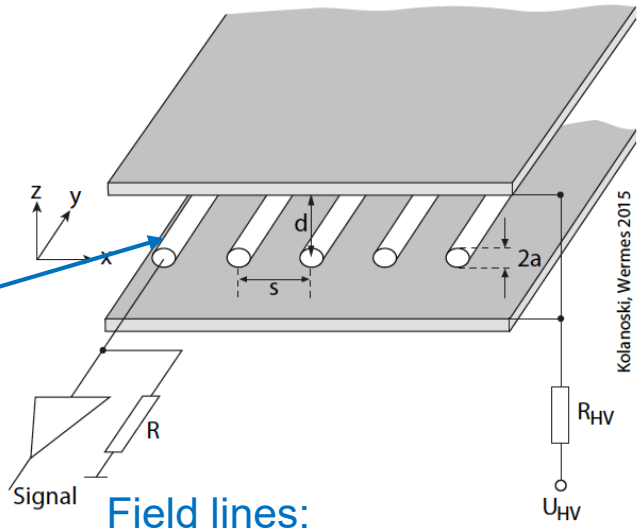

Thin anode wires – gas amplification

Field lines:
→ electrons guided to anodes

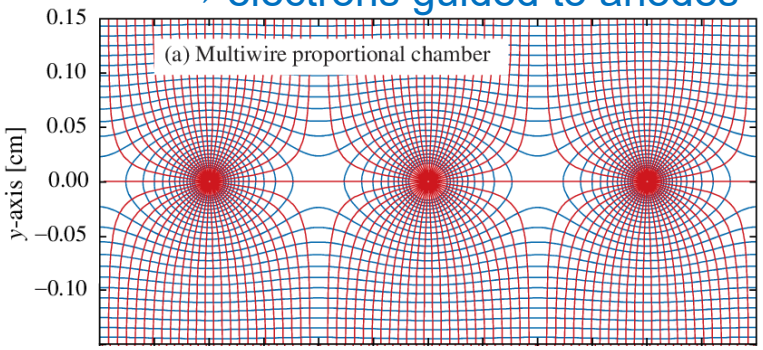

Charge particle ionizes the gas.
Electrons drift towards the anode.
For wire chambers, the anodes are realized by thin wires → amplification due to strong field.
Electronic processing of signal

Gas amplification:

Wire inside tube:

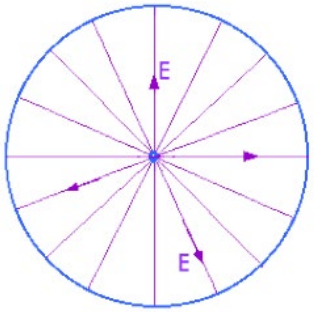

$$E(r) = \frac{U}{r \ln \frac{b}{a}}$$

b = radius of tube
a = radius of wire

Strong electrical field near the wire leads to acceleration of primary electrons and to further ionization → avalanche: gas amplification. Typ. gain ~10^5

Drift-chambers:

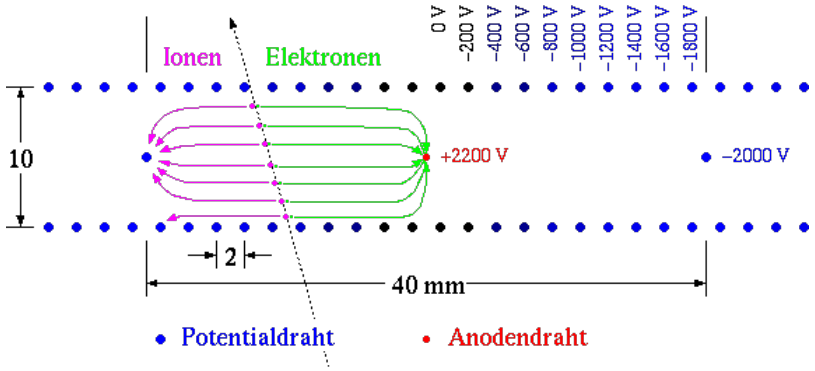

http://ikpe1101.ikp.kfa-juelich.de/

Drift chamber principle was established first in Heidelberg (Physikalisches Institut, by A. H. Valenta).

Using special wire configurations one can construct “drift cells” with very homogenous drift paths → one can use the drift time to reconstruct the particle trajectory.

Instead of building drift cells from complicated wire configurations simple tubes with an anode wire can be used:

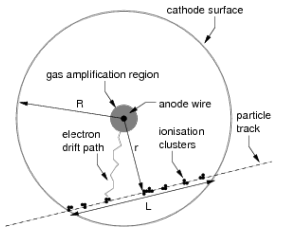

Example 1: JADE Jet-Chamber

Inner Radius: 20cm
Outer Radius: 80cm
Length: 2.4m

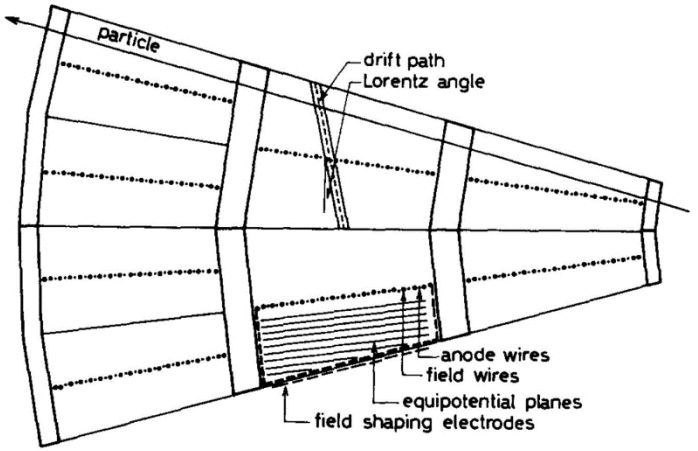

Spatial resolution rφ: 170 μm

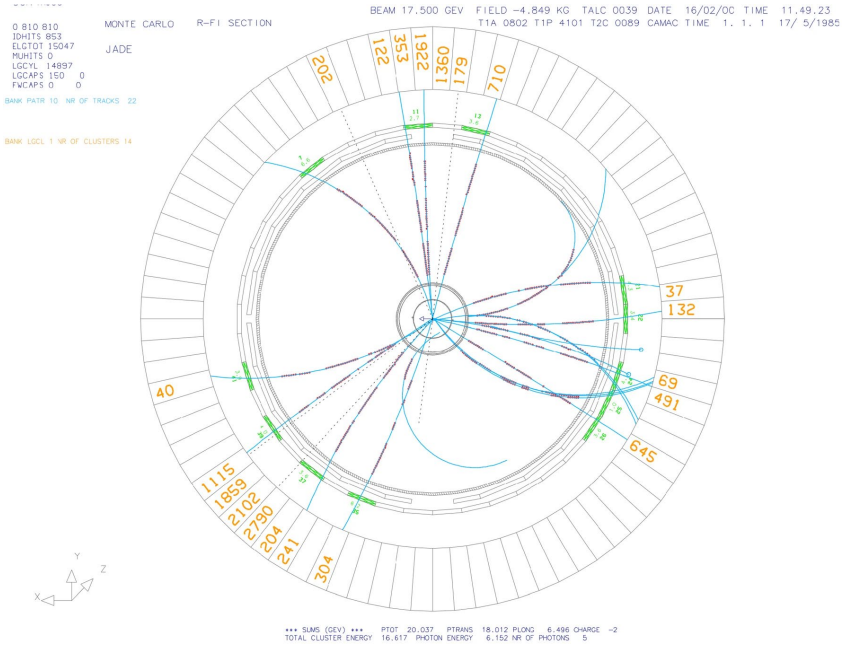

J. Heintze et al.
https://doi.org/10.1016/0029-554X(82)90658-9

Example 2: LHCb Outer Tracker

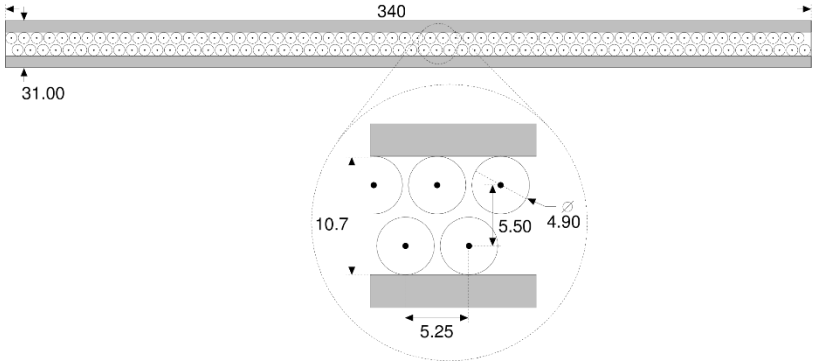

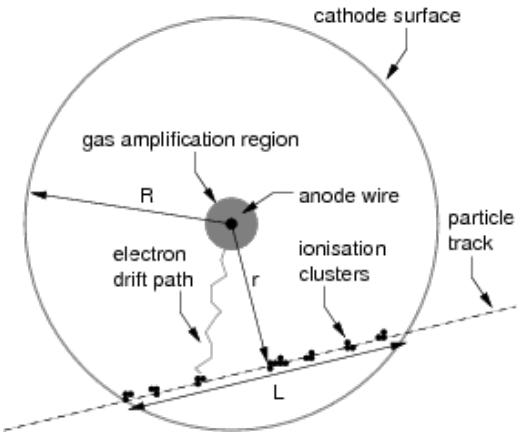

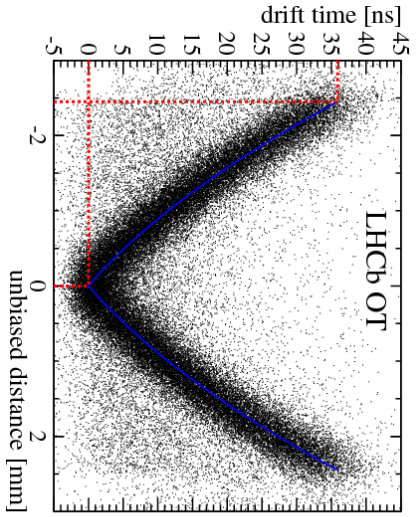

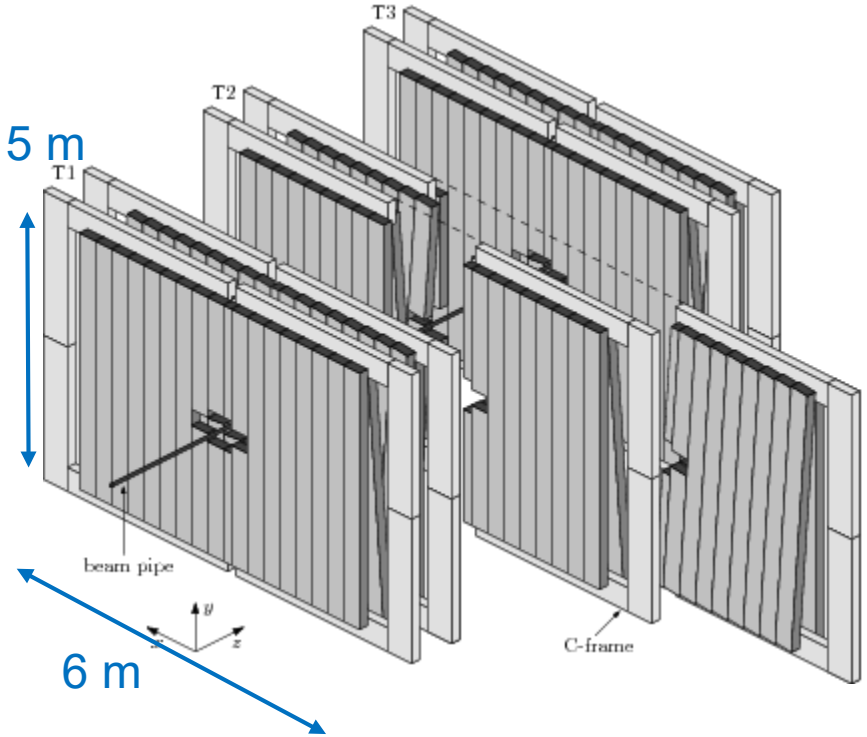

170 μm resolution over
360 m^2 detection areas

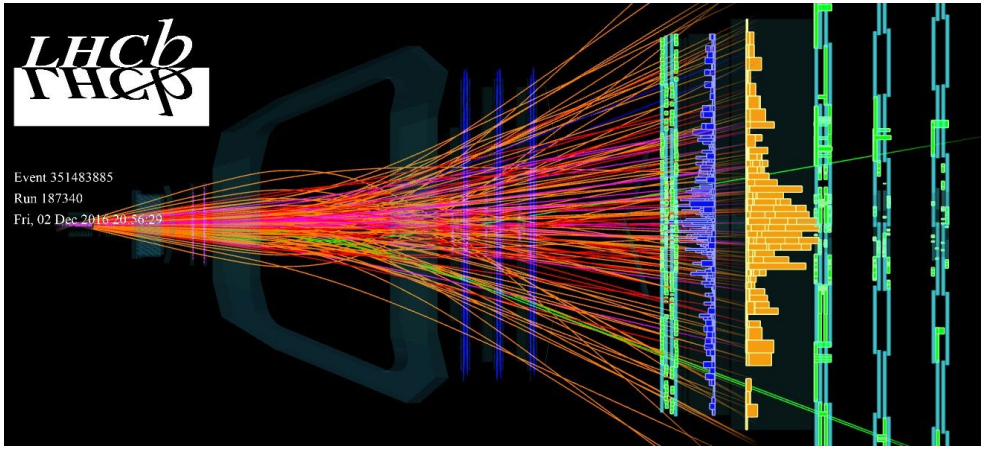

Semiconductor strip & pixel detectors

Semiconductor detector – based on depleted np-junctions (diodes)

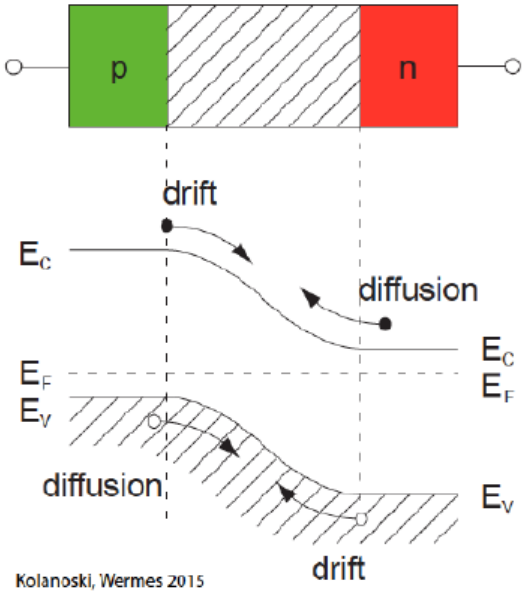

In the junction of p(n) doped semicondutors, the majority charge carriers will diffuse into the other region until the Fermi level is equalized.

Around the junction, there is a region w/o free charge carriers: depletion zone. A space charge is created (pos / neg one n / p-side).
The related electrical field produces a drift of charge carriers which compensates the diffusion.

The depletion zone can be enlarged by applying an external voltage:

With p-doping larger than n-doping, the depletion zone extends mostly into n:

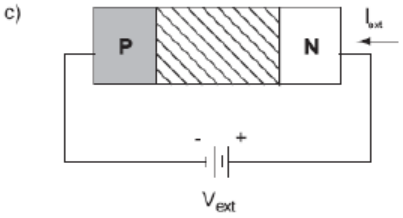

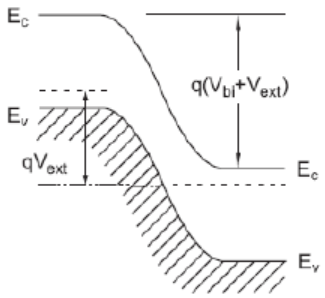

"reverse biasing"

Size of depletion zone:

$$d \approx x_n \approx \sqrt{\frac{2\epsilon\epsilon_0}{e}\frac{1}{N_D}(U_{bin}+U_{ext})}$$

$$\approx 3.6 \cdot 10^3 \sqrt{\frac{U_{ext}}{N_D(\mathrm{V\,cm})}}$$

~300 μm reachable

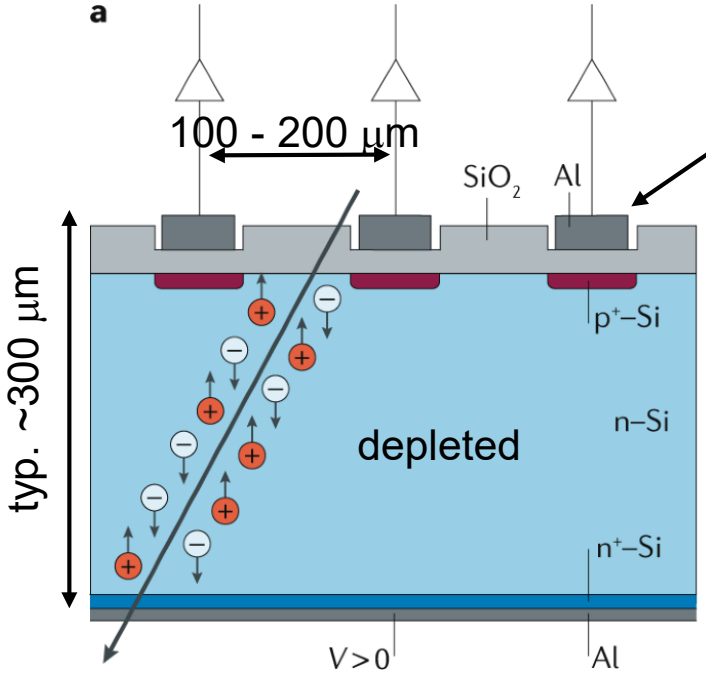

typ. strip length (into the figure plane) is O(10cm)

Schematics of a silicon strip sensor:

Strongly doped p^+-strips w/ aluminum contacts on weakly doped n-bulk which has an aluminum contact (by technical reasons there is a thin layer of strongly doped Al in between). Charge carriers (electrons) created by particles drift in the applied field to the p+ strips where they are detected.

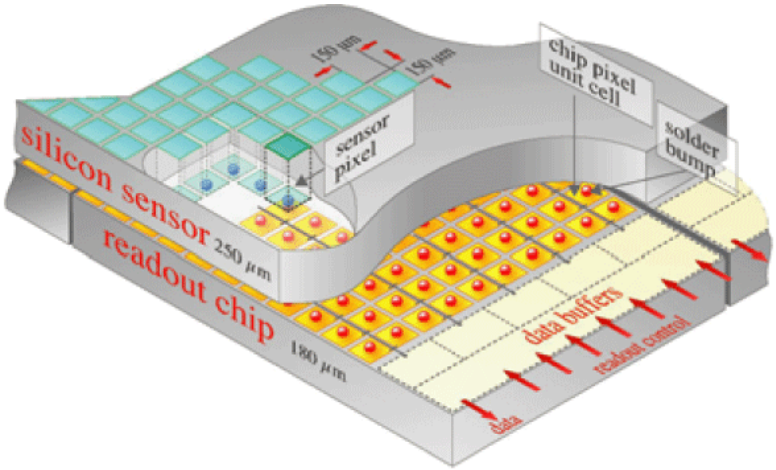

Schematics of a pixel sensor:

Instead of strips one uses small pixels typ. size 50 x 200…400 μm^2.

Challenge: Readout of the individual channels (please don't conclude from your phone camera – these devices are really very slow) . Requires a readout chip bonded to the pixel matrix: Hybrid pixel detectors.

Novel development: Monolithic pixel sensors with part of electronics in pixel matrix.

(→Heidelberg: Mu3ePix and MightyPix).

Example 1: CMS Tracker

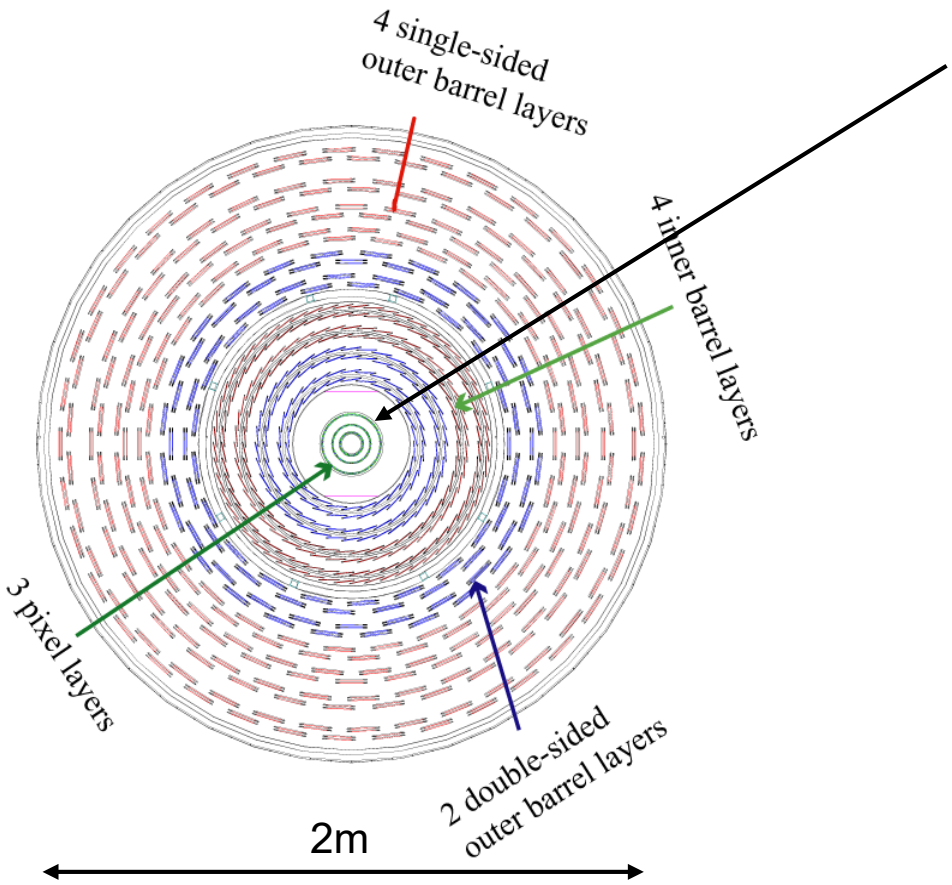

Silicon Pixel detector:
about 66 million 100×150 μm^2 pixels arranged at distance of 4 to 11 cm

Silicon strip detectors:
divided in the inner barrel part (TIB), the inner disks (TID), the outer barrel (TOB) and outer end-caps (TEC).

Tracker contains 15,200 sensitive modules with a total of about 10 million detector strips.

Strip distance = 80 μm to 200 μm
w/ strip widths about 25%

Spatial resolution: 20 – 30 μm

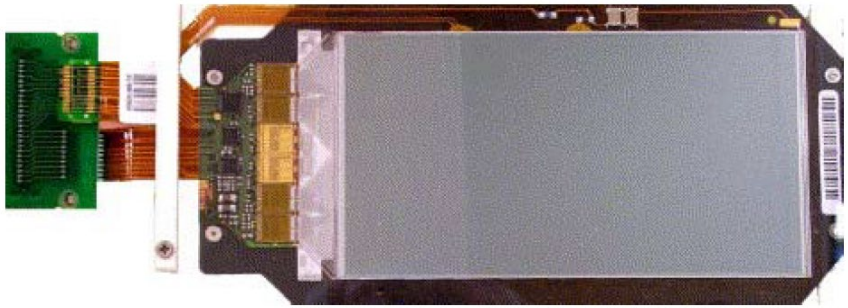

CMS TIB silicon strip modules.

Example 2: ATLAS Inner Tracker

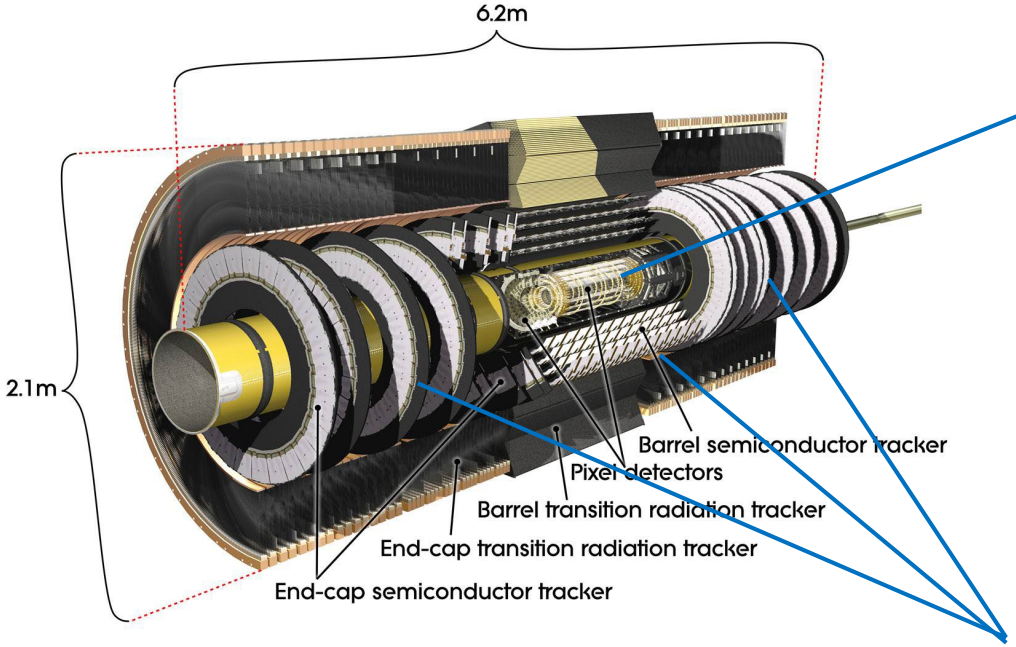

ATLAS pixel detector:

- 92 million pixels (92 million electronic channels).
- Silicon area approx. 1.9m^2
- Pixel 50 x 400μm^2 and 50 x 250 μm^2 for outer / inner external
- 4-barrel layers with 1736 modules
- 3 disks per end-cap w/ 288 modules
- Typ. Spatial resolution: 10 μm

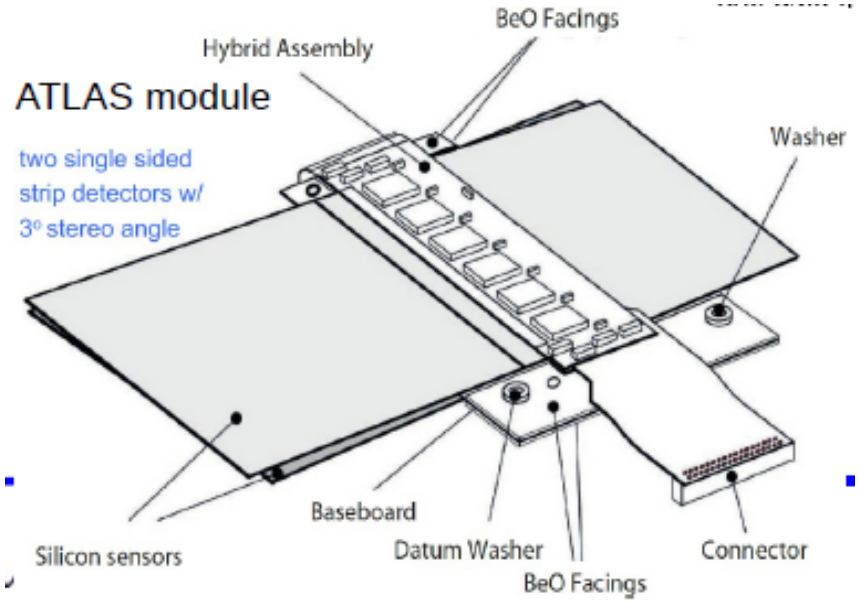

ATLAS strip detector:

4,088 two-sided modules and over 6 million implanted readout strips (6 million channels) 60m^2 of silicon distributed over 4 cylindrical barrel layers and 18 planar endcap discs Readout strips every 80μm.

Typ. spatial resolution: 25 μm

Momentum measurement and B field configurations

B-field (perpendicular w/ measurement plane)

Solenoid:

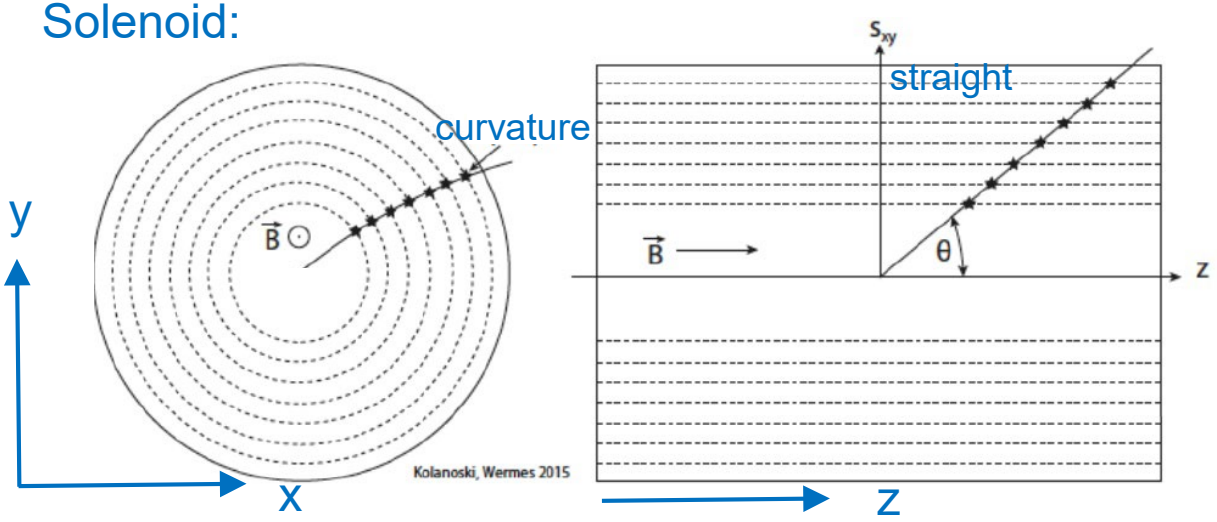

Lorentz force:

$$\vec{F}_{Lorentz} = q\left(\vec{v} \times \vec{B}\right)$$

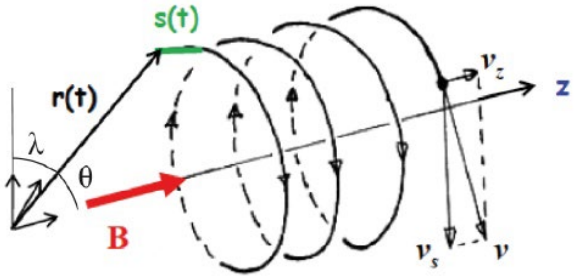

Particle moves on a helical trajectory

Curvature 1/R in xy-plane and particles transverse momentum p_T (within xy plane):

$$p_\perp = q \cdot B \cdot R \quad \text{or} \quad p_\perp[\mathrm{GeV}] = 0.3 \cdot B[\mathrm{T}] \cdot R[\mathrm{m}]$$

The momentum of the particle is obtained from p = p_T / cos θ

.How well can the transverse momentum be measured? What is its error?

Forward spectrometer configuration (fixed target exp. or forward experiments e.g. LHCb)

Dipole:

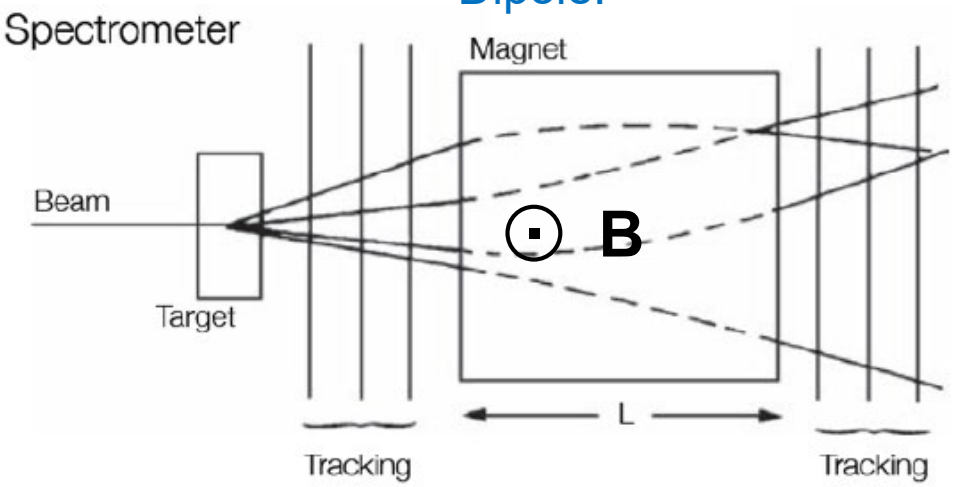

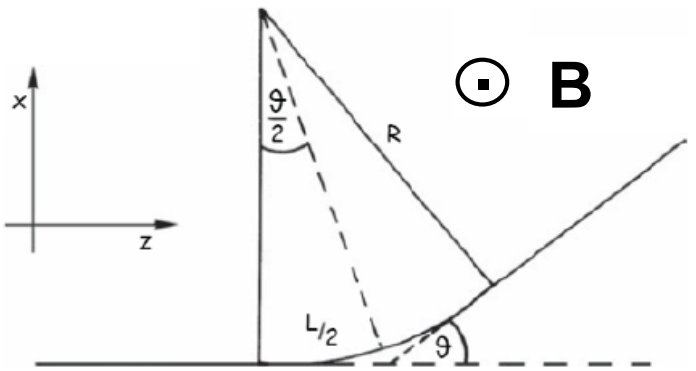

Minimum spectrometer configuration: 2 tracking station before and after magnet
3rd station is used for redundancy, fake rejection

Deflection angle ($p_T \perp B$)

$$\theta \approx \frac{L}{R} = \frac{L}{p_T}\, eB \quad \rightarrow p_T = \frac{eBL}{\theta} = \frac{0.3B[\mathrm{T}]L[\mathrm{m}]}{\theta}$$

$$\rightarrow dp_T = \frac{eLB}{\theta^2} d\theta = \frac{p_T}{\theta} d\theta \quad \rightarrow \frac{dp_T}{p_T} = \frac{d\theta}{\theta}$$

Relative momentum resolution is given by relative angular resolution (depends on spatial resolution of tracker)

Deflection results into momentum-kick Δp_x :

$$\Delta p_x = p_T \sin\theta \approx p_T\, \theta = eBL$$

often called bending power

Assume the minimum tracker configuration w/ 2 + 2 tracking stations w/ spatial resolution σ_x

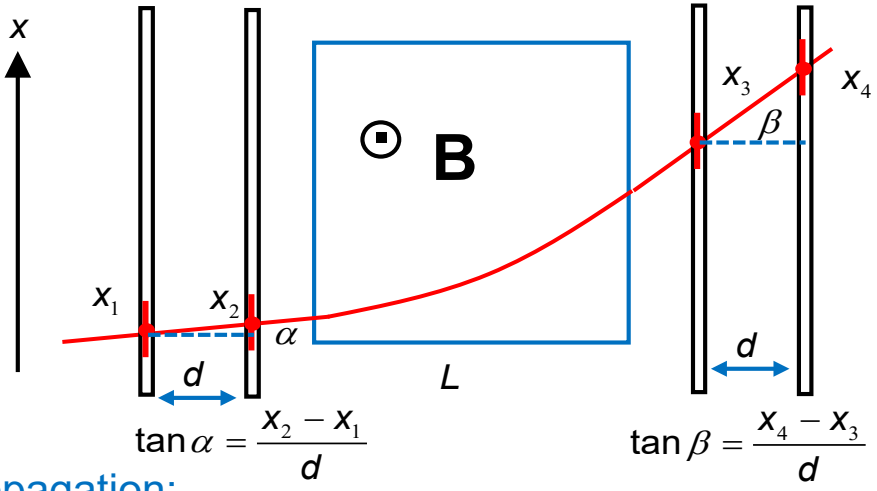

deflection $\theta = \beta - \alpha \approx \tan\beta - \tan\alpha$

$$\theta \approx \frac{x_4 - x_3}{d} - \frac{x_2 - x_1}{d}$$

W/ σ_x same for all layers, one obtains w/ error propagation:

$$d\theta = \frac{2\sigma_x}{d} \quad \text{and with} \quad \frac{dp_T}{p_T} = \frac{d\theta}{\theta}$$

$$\frac{dp_T}{p_T} = \frac{p_T}{eBL}\frac{2\sigma_x}{d} = \frac{p_T}{0.3B[T]L[m]}\frac{2\sigma_x}{d}$$

with $p\theta = eBL$

For N points before and after magnet: $d\theta = \frac{\sigma_x}{d}\sqrt{\frac{24(N-1)}{N(N+1)}}$

Relative momentum resolution depends on p. Improves for larger field integral BL and larger Measurement "arm" h.

There is also a uncertainty on θ from multiple scattering inside the plane:

$$\sigma_{p,MS} = p\sin\theta_{0,MS} \approx p\theta_{0,MS} = p\cdot\frac{13.6\text{MeV}}{\beta p}\sqrt{\frac{L'}{X_0}} = 13.6\text{MeV}\sqrt{\frac{L'}{X_0}}$$

Should consider sum of all materials

Contribution to p resolution results from the comparison w/ p-kick and bending power:

$$\frac{\sigma_{p_T,MS}}{p_T} = \frac{\sigma_{p_T,MS}}{\Delta p_x}_{\text{p-kick}} = \frac{13.6\text{MeV}}{eBL}\sqrt{\frac{L'}{X_0}}$$

Contribution from multiple scattering to relative resolution has no momentum dependence

Momentum resolution considering detector spatial resolution and multiple scattering is given by:

$$\left.\frac{\sigma_{p_T}}{p_T}\right|_{tot} = \sqrt{\left(\left.\frac{\sigma_{p_T}}{p_T}\right|_{det}\right)^2 + \left(\left.\frac{\sigma_{p_T}}{p_T}\right|_{MS}\right)^2}$$

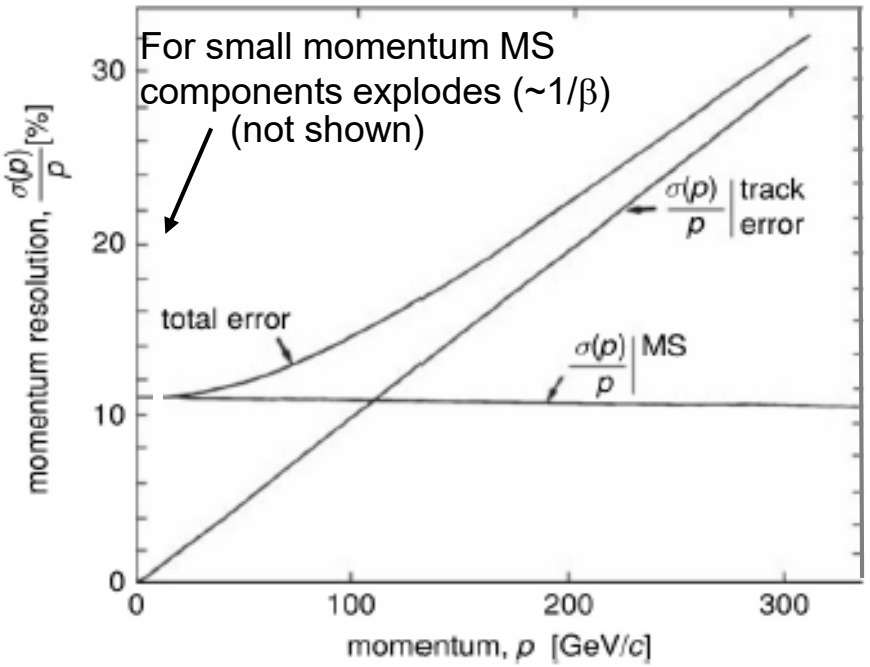

This formula can be applied to more complicated cases – e.g. measurement of the track curvature be cylindrical tracking detector. Assuming the curvature is measured by N space points over distance L one finds for the detector resolution:

$$\left.\frac{\sigma_{p_T}}{p_T}\right|_{det} = \frac{p_T}{0.3}\frac{\sigma_{Hit}}{BL^2}\sqrt{\frac{720}{N+4}} \quad \text{for } N \geq 10$$

(B in T, L in m, p in GeV)

(In literature referred as Gluckstern formula)

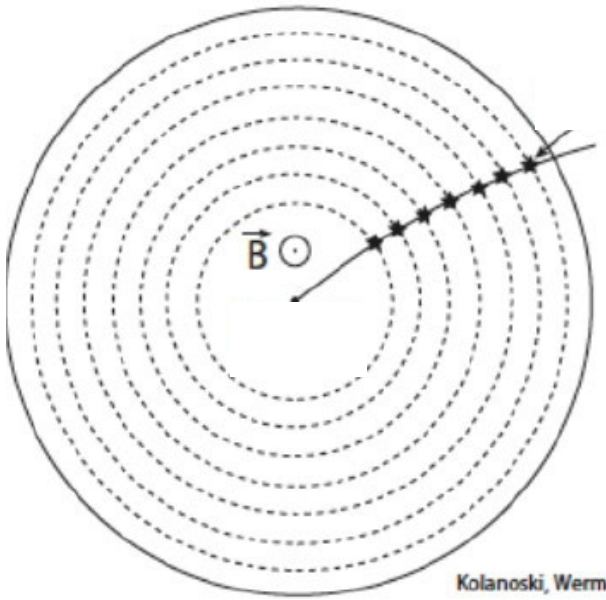

Track reconstruction:

Track reconstruction is usually split into two separate steps:

- **Pattern recognition**: detector hits (space points) are assigned to individual tracks
- **Fit of track model** to space points, accounting for resolution & multiple scattering

Pattern recognition: here w/ local tracklets

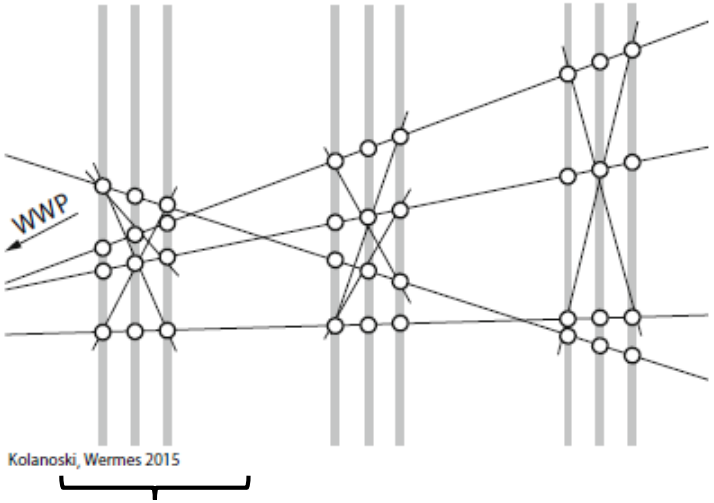

Find locally all possible combinations (tracklets)

Combine local stubs to global tracks

Fit the hits of tracks by a track model.
Often: Kalman filter fit to consider scattering and refine track model.

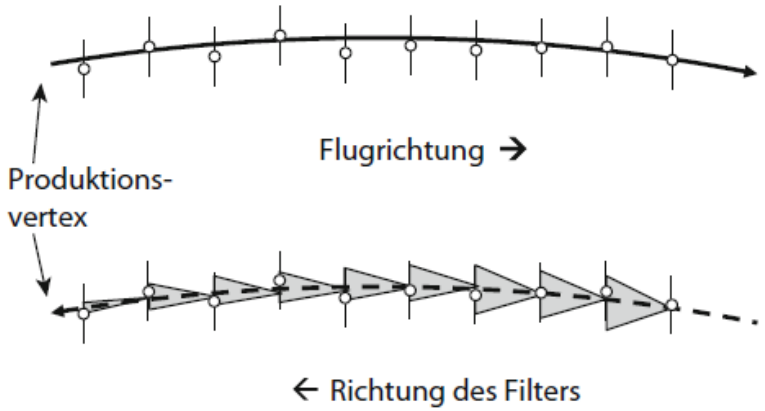

In this way the track model at the last point (close to vertex) is optimized and allows best prediction of vertex.

Tracking detector layout optimized to allow fast and efficient pattern recognition and very good prediction of the vertex from the fitted track model at the last hit.

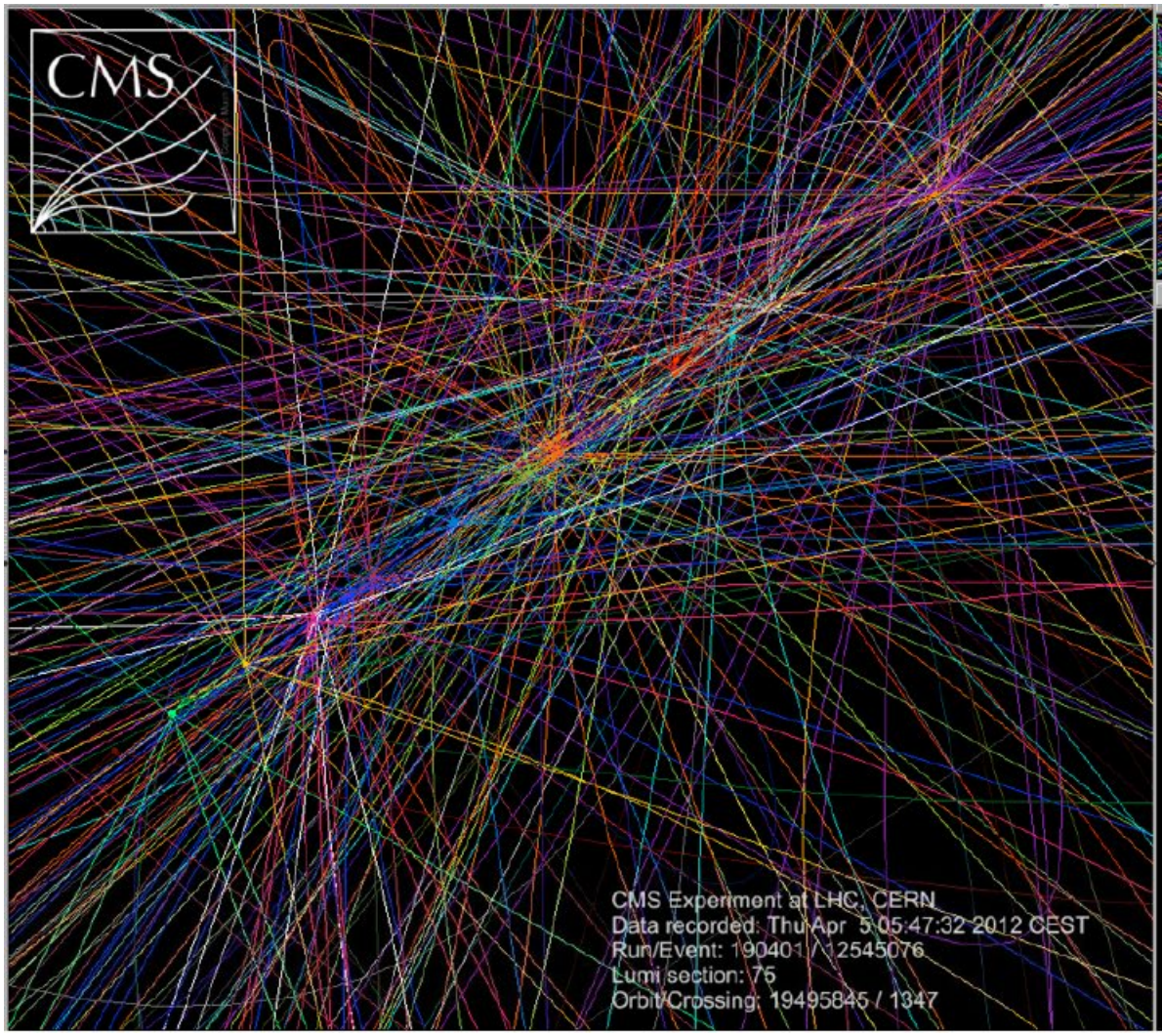
CMS
CMS Experiment at LHC, CERN
Data recorded: Thu Apr 5 05:47:32 2012 CEST
Run/Event: 190401 / 12545076
Lumi section: 75
Orbit/Crossing: 19495845 / 1347

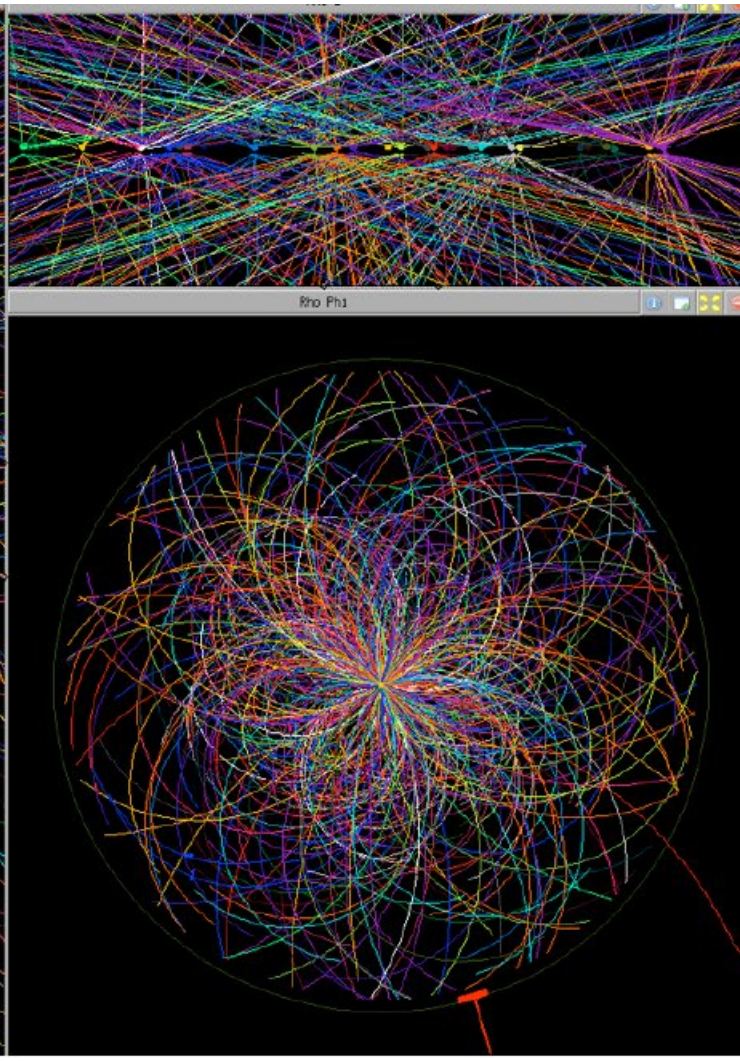
Rho Phi

3. Calorimeters – energy measurement

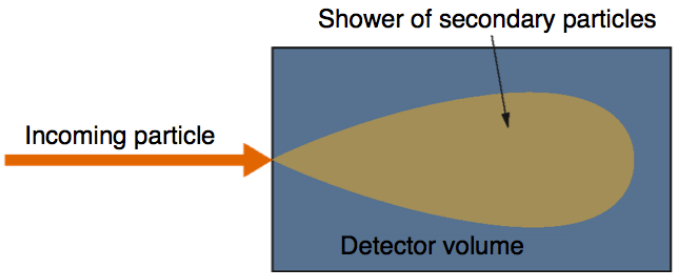

Particle to measure shower (secondary particles) and deposit their whole energy into the detector volume,

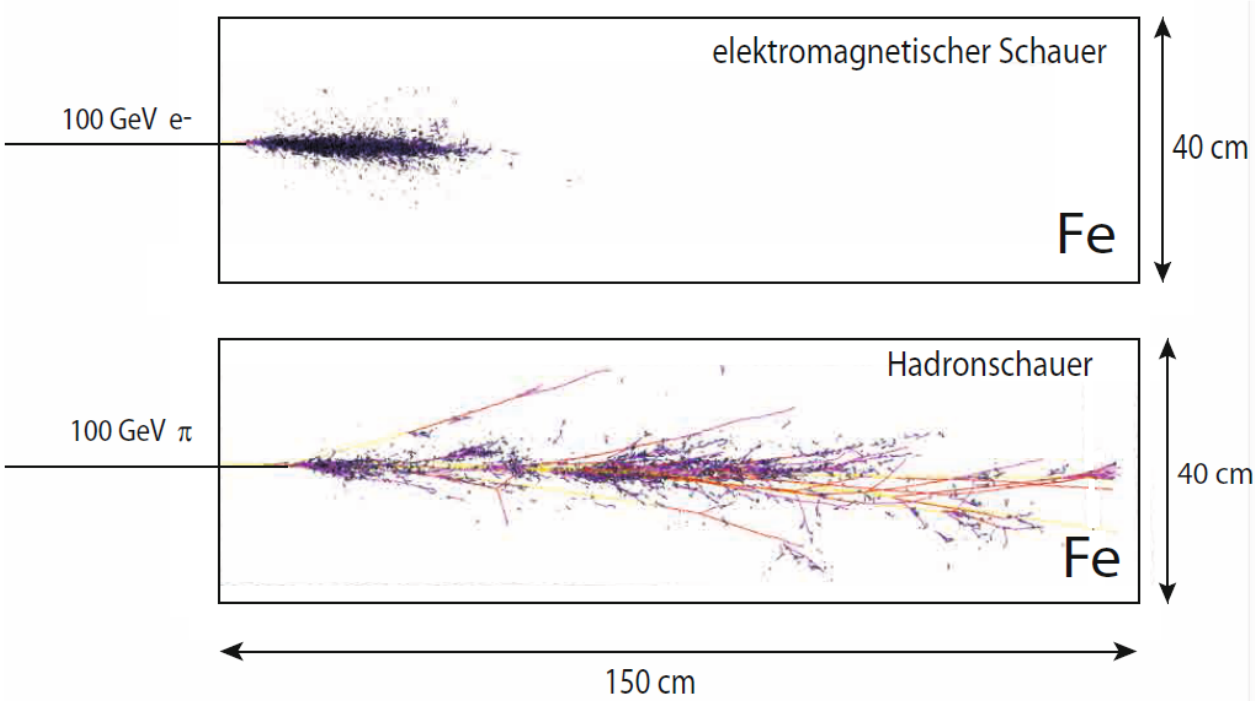

Electromagnetic shower: length scale determined by radiation length

Hadronic shower: length scale determined by hadronic interaction length (much larger)

Because of the very different shower development one distinguishes between electromagnetic calorimeters (ECAL) to measure electrons and photons and hadronic calorimeters (HCAL) to measure the energy of hadrons and jets.

Two types of calorimeters:

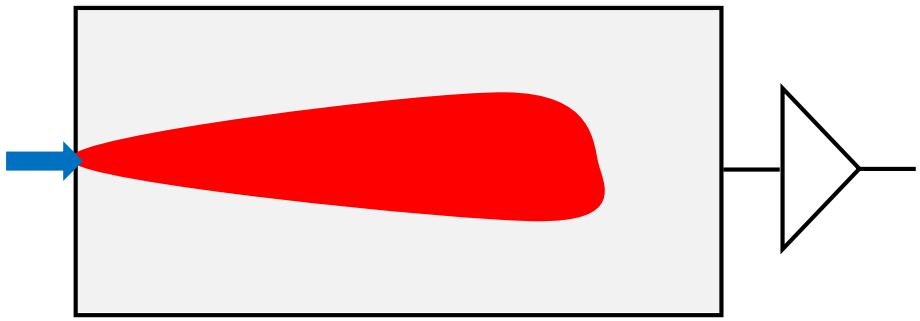

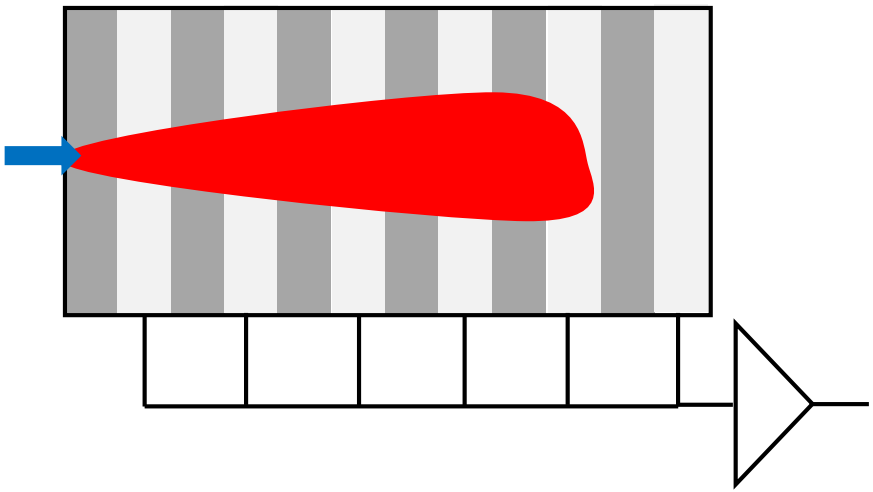

Homogenous calorimeters:

- "Absorber" / shower material is active and provides a measurable signal.
- All the deposited energy is transferred into the signal → best possible resolution.
- expensive
- Used only for "compact" electromagnetic calorimeters.

Sampling calorimeters:

- "Absorber" / shower material is not active and interleaved with active material (e.g. scintillators) to provide signals.
- Only a fraction of the deposited energy converted into signal → sampling fluctuations (degrades res.)
- Hadronic calorimeters (always) and electromagnetic calorimeters.

Homogenous calorimeter:

In homogenous calorimeter the active detector material and the absorbing material is the same. As these calorimeters are typically used for ECALs the material should have a large Z to keep the calorimeter compact ($X_0 \sim A/Z^2$).

The following detection mechanisms and materials are used:

Detection mechanism	Material
Scintillation	CsJ, BGO*), BaF_2, CeF_2, $PbWO_4$
Cherenkov light	Lead glass (OPAL exp.), water (Kamiokande)
Ionization	Liquid nobel gases (Ar, Kr, Xe), Semiconductors: Germanium

*) Bismuth Germanate $Bi_4\ Ge_3\ O_{12}$

Signal detection:

- Light of scintillators is read-out using photo-detectors: photo-multiplier tubes or silicon photo-multiplier (very cheap)
- Cherenkov light: photo-detectors
- Ionization: charge collection using E field to drift the charges to collecting electrodes

Example of homogenous electromagnetic calorimeter: Belle II calorimeter

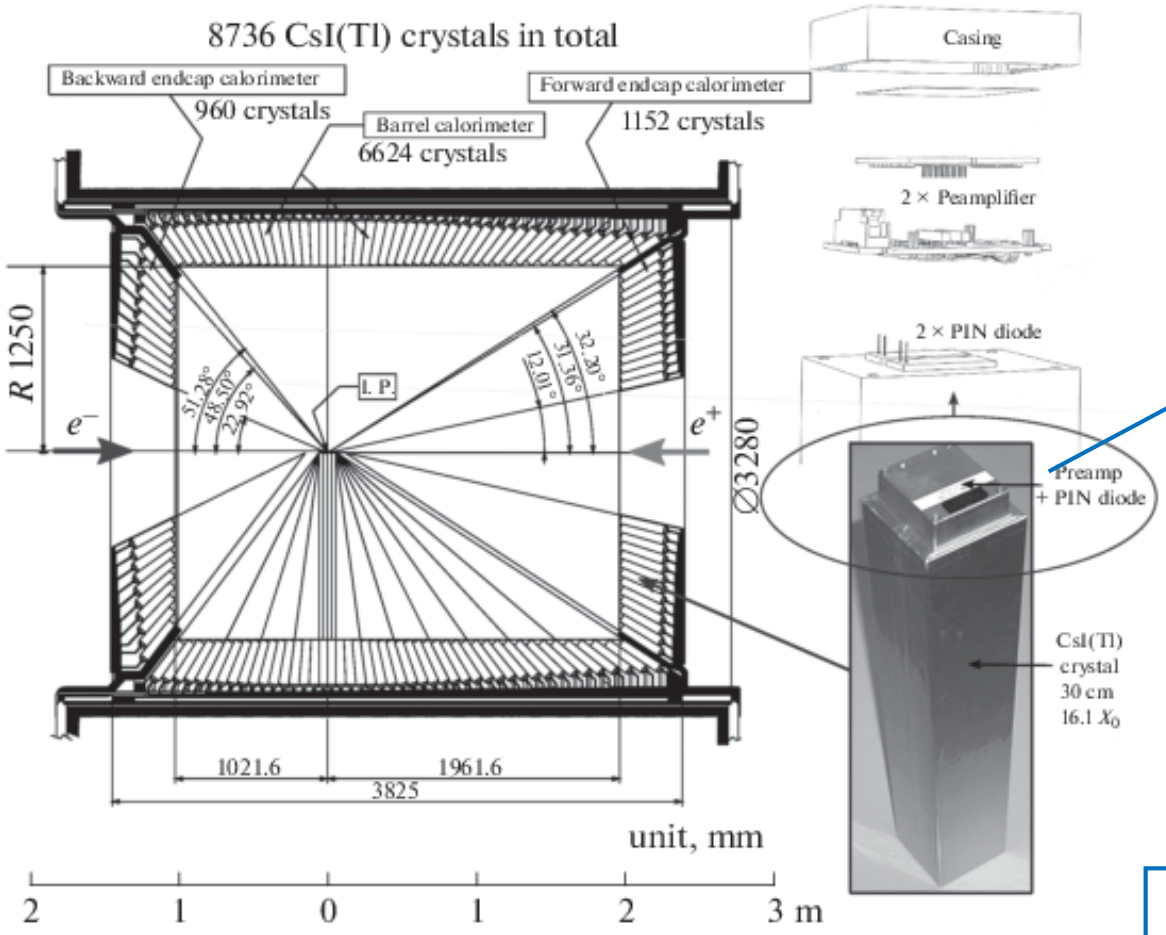

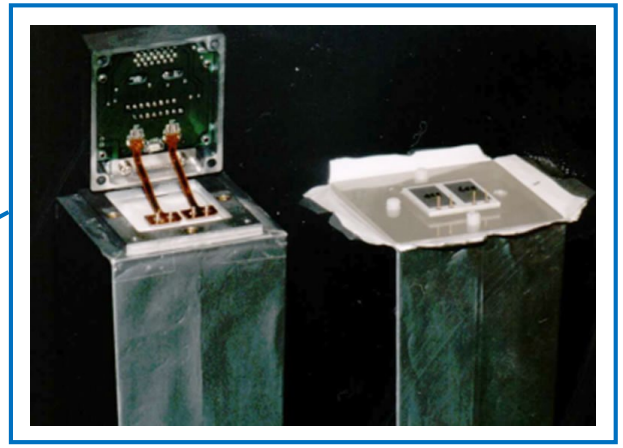

https://doi.org/10.1134/S1063779618040494

Resolution:
$\sigma E/E$ ~ 2% for E above 1GeV
σx : 5~10mm at incident point

Sampling calorimeter:

Advantages:
One can optimally choose the absorber and detection material independently and according to the application. By choosing a very dense absorber material the calorimeters can be made very compact. The passive absorber material is cheap

Disadvantages:
Only part of particles energy is deposited in the detection layers. Measured energy resolution is worse than in homogenous calorimeters (“Sampling-Fluctuations”)

Scintillators:

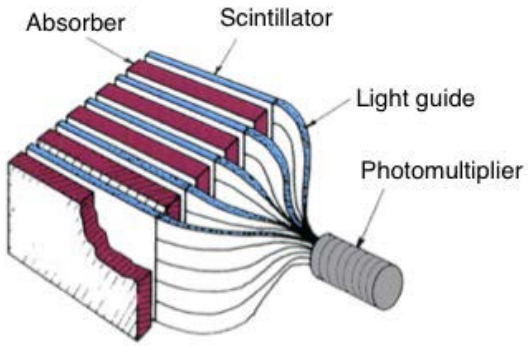

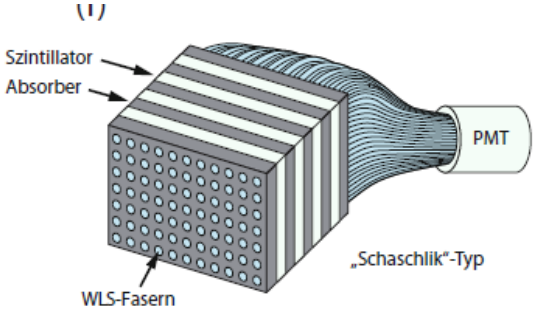

Kolanoski, Wermes 2015

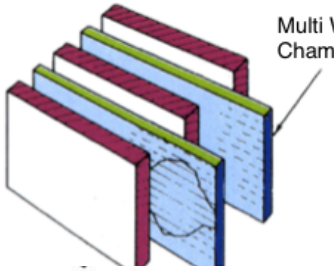

Wire chambers

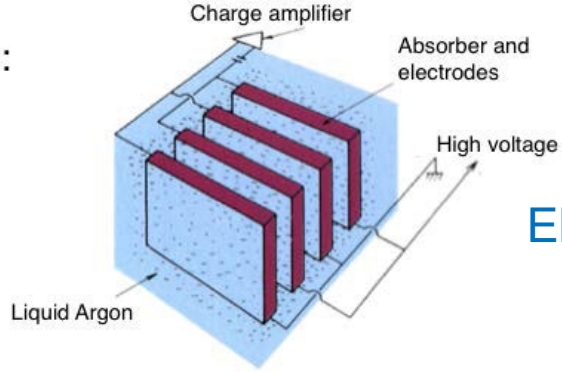

Electrodes

Example: ATLAS Calorimeter System

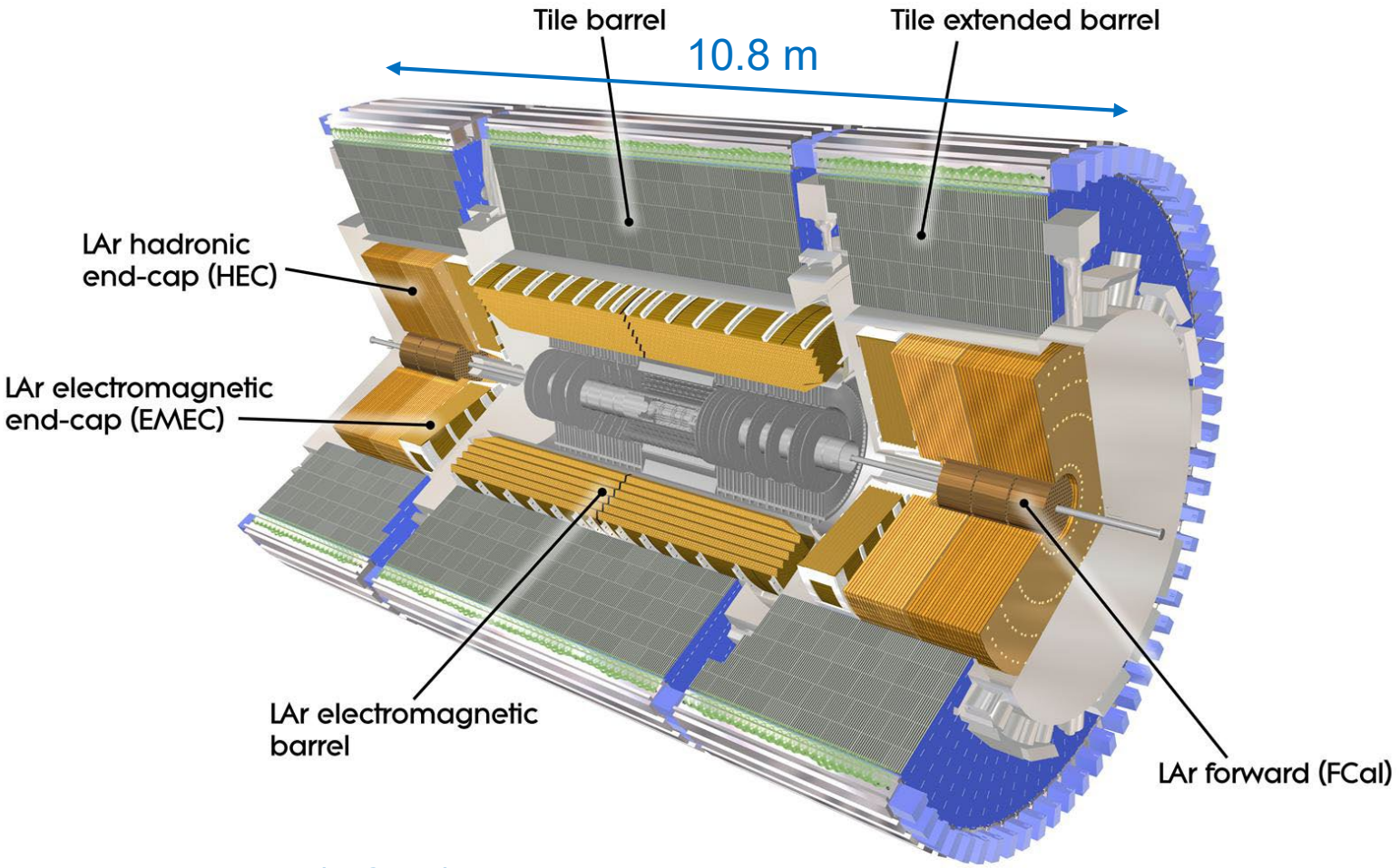

Barrel LAr calorimeter (ECAL):
6.4 m long, 53 cm thick, 110 000 channels

Tile calorimeter (HCAL):
500000 scintillator tiles

LAr Electromagnetic Calorimeter:

Absorber: thin lead plates in accordion structure in LAr as active material.

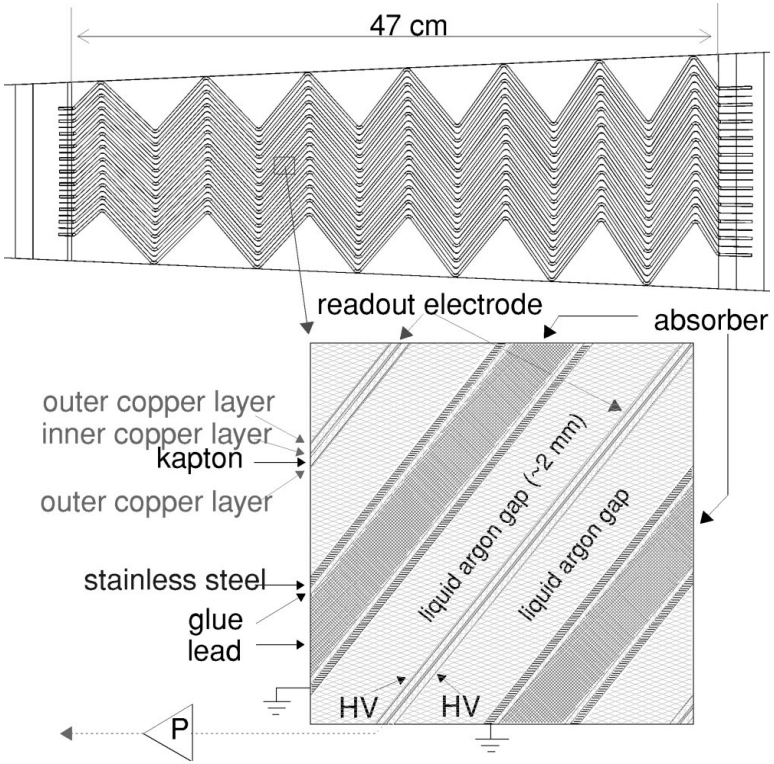

$$\frac{\sigma_E}{E} = \frac{10\%}{\sqrt{E}} \oplus \frac{2\%}{E} \oplus 0.2\%$$

Noise term at larger energies negligible.

Tile Hadron Calorimeter:

Iron (absorber) tiles and plastic scintillator tiles as active detector.

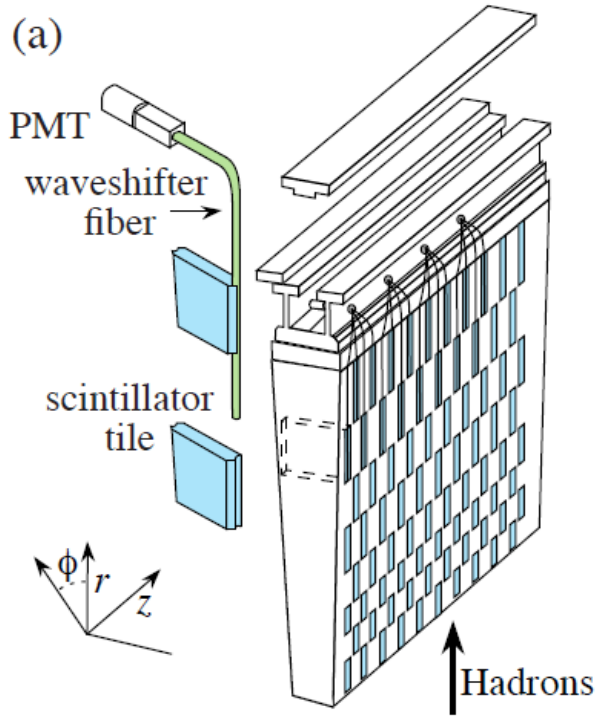

$$\frac{\sigma_E}{E} \approx \frac{45\%}{\sqrt{E}} \oplus \frac{2..5\%}{E}$$

For hadrons w/ E=16…30GeV

https://arxiv.org/pdf/2102.04088

Electromagnetic shower: (see simple shower model)

Using detailed Monte Carlo simulations:

Shower maximum in units of X_0:

$$t_{\max} = \ln\left(\frac{E}{E_c}\right) + B$$

B=-0.5 for $e^{\pm}$, B=+0.5 for γ

95% longitudinal shower containment

$$t_{95\%} = t_{\max} + 0.08Z + 9.6$$

Rule of thumb: ~25 X_0

95% lateral shower containment:

$$R_{95\%} = 2\rho_M$$

Longitudinal and lateral shower development:

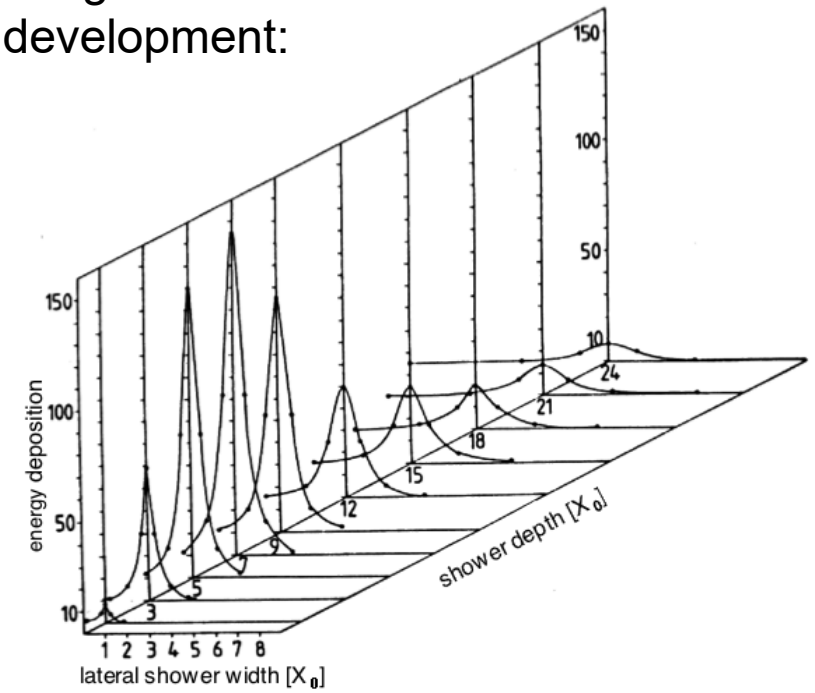

Moliere radius ρ_M: $\rho_M \approx \frac{21\text{MeV}}{E_c} X_0$

Material	X_0 [cm]	ρ_M [cm]
Fe	1.76	1.77
Pb	0.56	1.60
U	0.32	1.00

Energy resolution of electromagnetic calorimeters:

Intrinsic resolution (homogeneous calorimeter)

In an ideal homogenous calorimeter the energy resolution is determined by the statistical fluctuations of the number of detectable signal particles N ~ E:

$$\frac{\sigma_E}{E} \sim \frac{\sigma_N}{N} \approx \frac{\sqrt{N}}{N} = \frac{1}{\sqrt{N}} \sim \frac{1}{\sqrt{E}}$$

Usually called "stochastic term"

Sampling fluctuations (sampling calorimeters):

In sampling calorimeters only a small part of the deposited energy is measured. The fractions of how much energy is deposited in the absorber and in the active detector varies from event to event → these fluctuations cause a degradation of the energy resolution:

$$\frac{\sigma_E}{E} \sim \sqrt{\frac{\Delta E}{E}}$$

ΔE is the average energy deposition in an absorber layer, ratio is a measure of number of samplings (the higher, the better)

Sampling fluctuations: $\frac{\sigma_E}{E} \sim \frac{1}{\sqrt{E}}$

Additional contributions (for real calorimeters):

- Noise in the detector or the electronics N_{noise} → fake energy: $E_{fake} \sim N_{noise}$

  Effect on resolution: $\frac{\sigma_E}{E} \sim \frac{1}{E}$

- Constant term; Channel-to-channel response calibration: $\frac{\sigma_E}{E} \sim C$

Parametrisation of the energy resolution of a real calorimeter:
The total energy resolution is the quadratic sum of different contributions

$$\frac{\sigma_E}{E} \sim \sqrt{\left(\frac{b}{E}\right)^2 + \left(\frac{a}{\sqrt{E}}\right)^2 + c^2}$$

$$\frac{\sigma_E}{E} \sim \frac{a}{\sqrt{E}} \oplus \frac{b}{E} \oplus c$$

$\oplus$ =quadratic sum

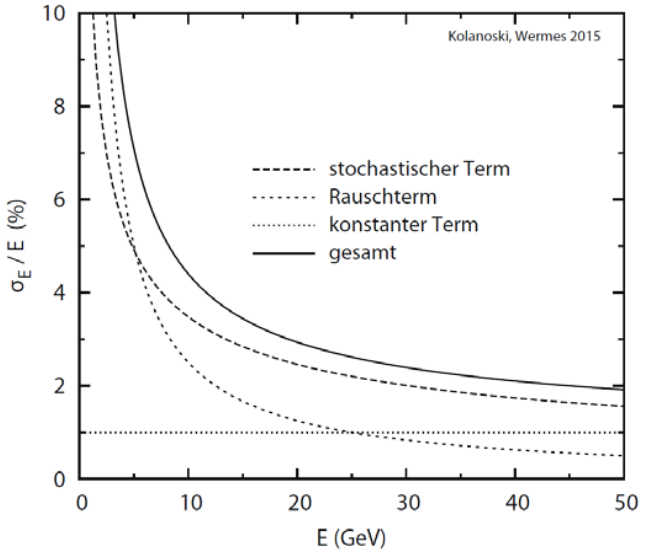

Different behaviour than spectrometer

Hadronic shower:

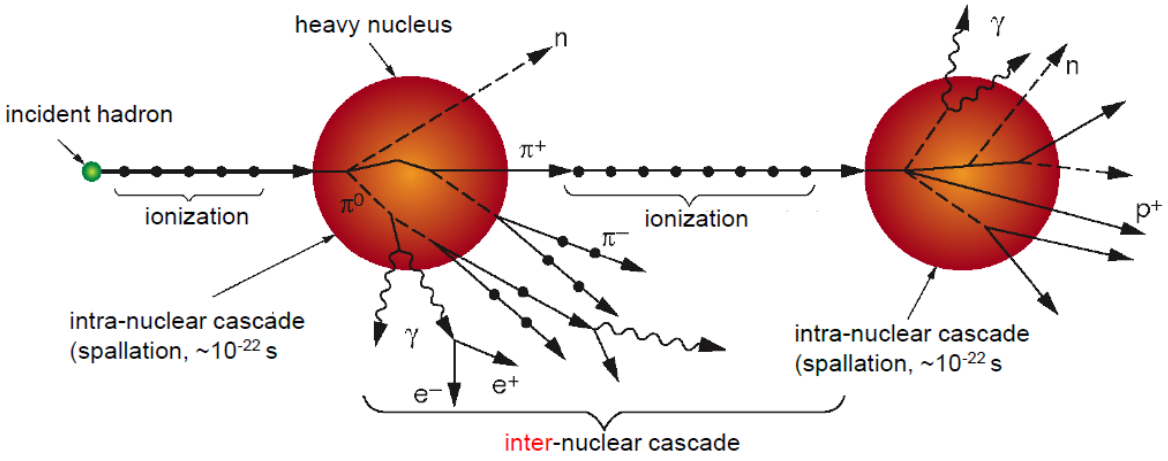

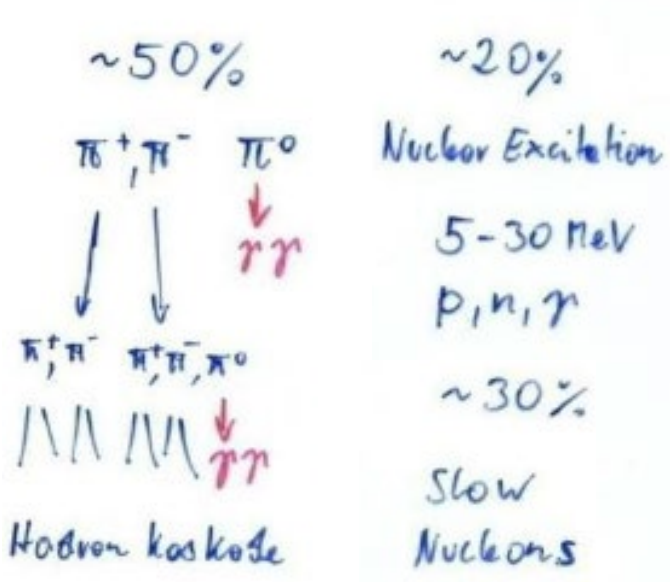

Significant fraction of deposited energy does not lead to a detectable signal in active detector: neutrons, K^0 , nuclear excitations, pion decays $\pi \rightarrow \mu\nu$ w/ minimal ionizing muons and undetectable neutrinos escaping the calorimeters.

Additional problem: fluctuating electromagnetic component from $\pi^0 \rightarrow \gamma\gamma$ decays.

e/h ratio (electromagnetic / hadronic response) :

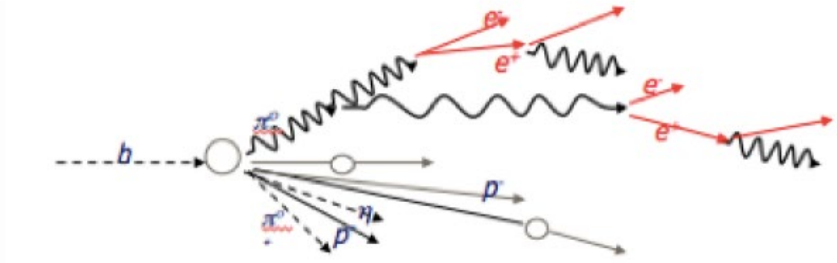

Electromagnetic component

Hadronic component

Large variations from event to event

10 GeV e/π → 

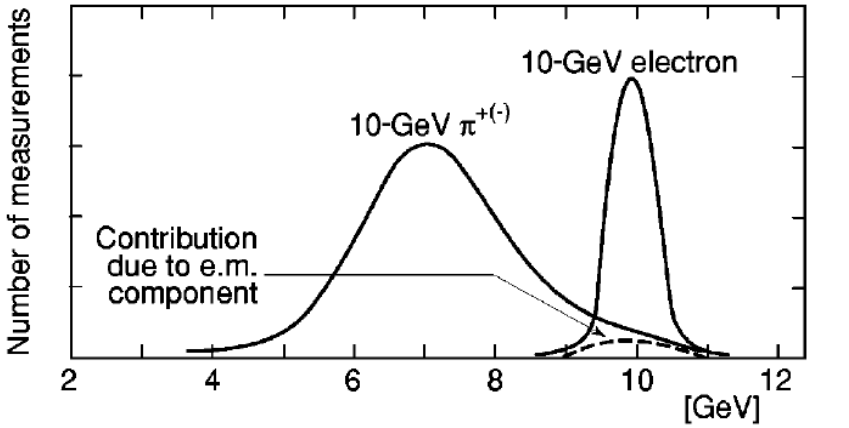

Signal (in energy units) obtained for a 10 GeV energy deposit

The electromagnetic component in a shower is over-weighted. To reduce the effect of fluctuation of the electromagnetic component people tried to build "compensated calorimeters" with an e/h ratio close to 1. E.g.: ZEUS uranium / plastic scintillator calorimeter (not too successful). Alternatively software compensation is used (needs longitudinal segmentation): works!

Energy resolution of hadron calorimeters:

A fluctuating e.m. shower component together with e/h ≠ 1, fluctuations in the shower composition w/ muon and neutrinos escaping the calorimeter, and undetected energy from neutrons and spallation leads to an energy resolution for hardon calorimeters which is significantly worse than the one for electromagnetic calorimeters.

For the stochastic term of HCALs one usually finds values of 40-60%/√E [GeV]

Shower containment:

Longitudinal shower extension:
For high energy hadrons 8…10 interaction lengths are needed to contain the shower

Lateral shower extension:
95% of shower contained within a cylinder with R≈1.5 λ_{int}

Reminder: λ_{int}(Fe) = 17 cm

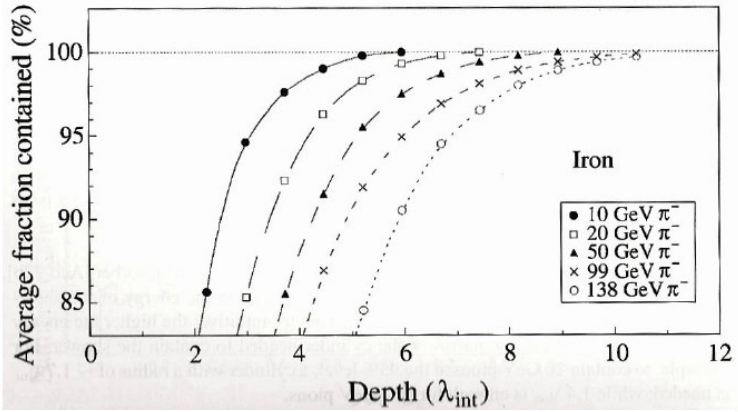

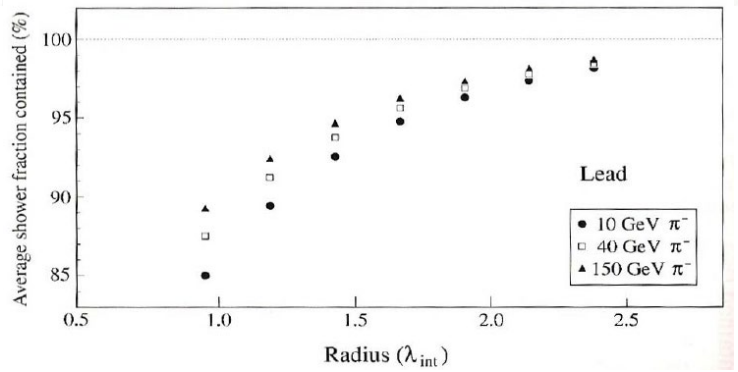

4. Particle identification (PID)

Specific signatures of photons, electrons, muons, charged hadrons, neutral hadrons:

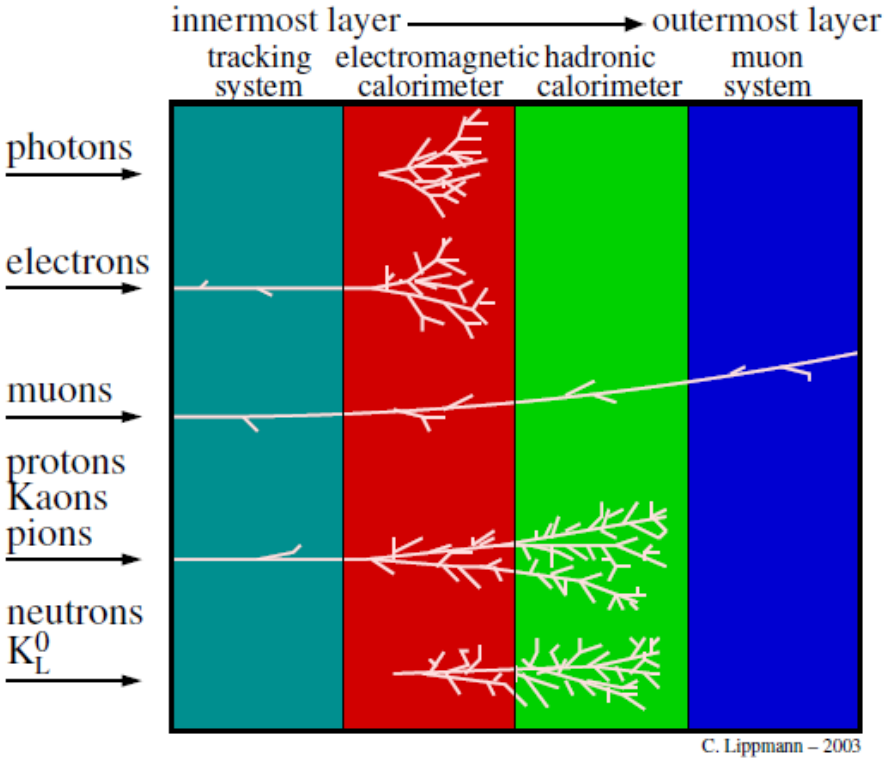

Particle identification using these signatures.

However, some experiments are also interested to distinguish **different charged hadrons:** K, π, p are "pseudo" stable and the end-product of many heavier hadron decays. To reconstruct these decays PID knowledge of their daughters (K, π, p) is necessary.

Hadron PID: (identification of p, K, π)

General idea: In addition to the measured particle's **momentum** one determines the particle's **velocity** (or the particle's $\beta\gamma$ value). An independent determination of momentum and velocity allows to estimate the **mass** of the particle.

Three different techniques are used to determine the particles velocity:

- Measurement of the specific energy-loss dE/dx from ionization
- Time-of-flight measurement for a given flight-distance
- Measurement of the angle θ_c of the of the Cherenkov light-cone

Specific energy-loss dE/dx

Specific energy loss of different particles as function of the particle momentum: see Bethe-Bloch formula

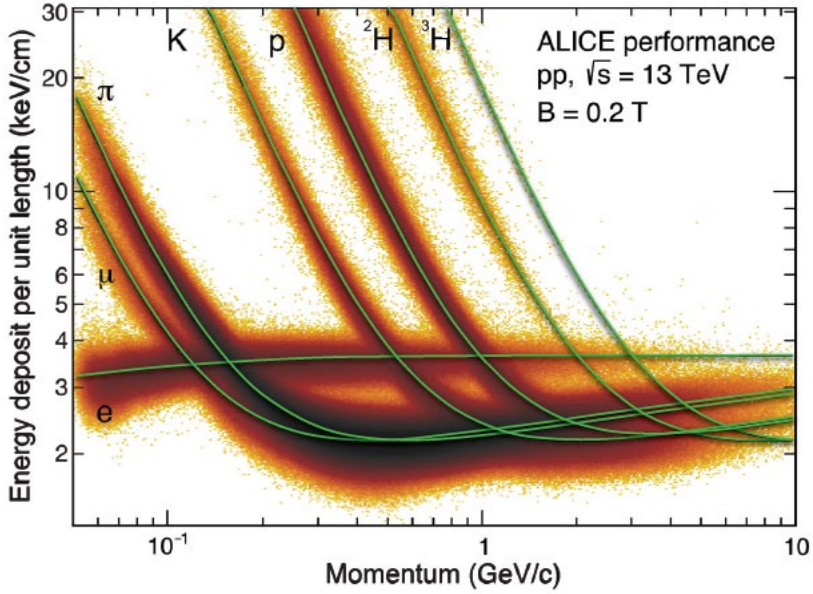

Figure 35.16: Energy deposit versus momentum measured in the ALICE TPC.

Time of flight measurement:

Time of flight (ToF)

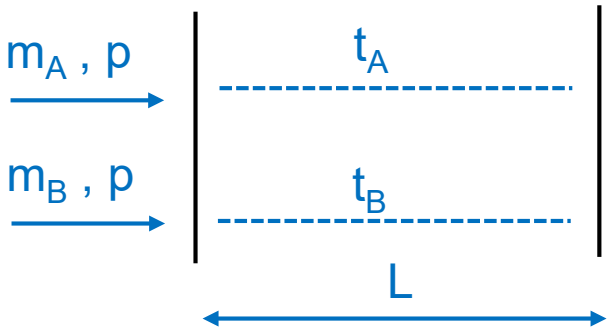

One finds w/ p=γβcm

$$m = \frac{p}{c}\sqrt{\frac{c^2t^2}{L^2} - 1}$$

$$|t_A - t_B| = \frac{L}{c}\left|\sqrt{1+\left(\frac{m_A c}{p}\right)^2} - \sqrt{1+\left(\frac{m_B c}{p}\right)^2}\right|$$

Assuming a finite time resolution σ_{TOF} and approximating $\sqrt{1+(mc/p)^2} \approx 1 + (mc)^2/2p^2$ for p >> mc, one finds for the separation in sigmas (n_σ):

$$n_{\sigma_{TOF}} = \frac{|t_A - t_B|}{\sigma_{TOF}} = \frac{Lc}{2p^2\sigma_{TOF}}|m_A^2 - m_B^2|$$

The plot shows for which momenta a separation between π/e, K/π, K/p is possible.

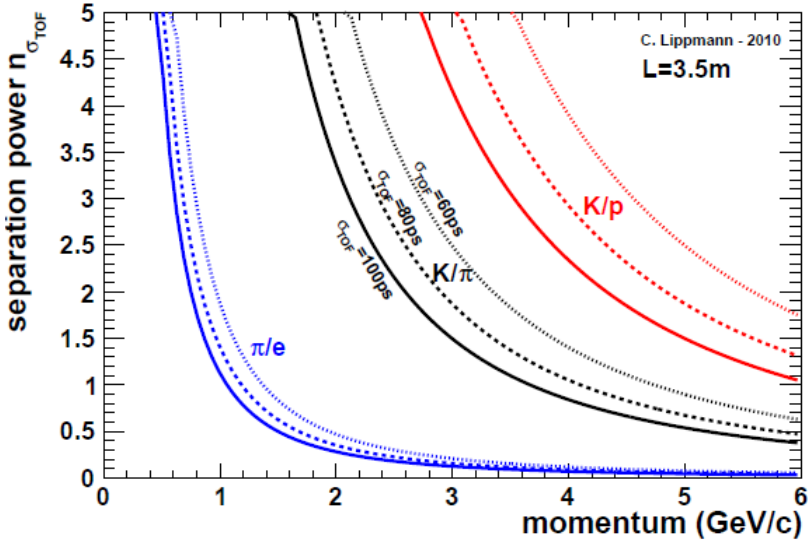

Example: ALICE TOF system

Multigap Resistive Plate Chambers

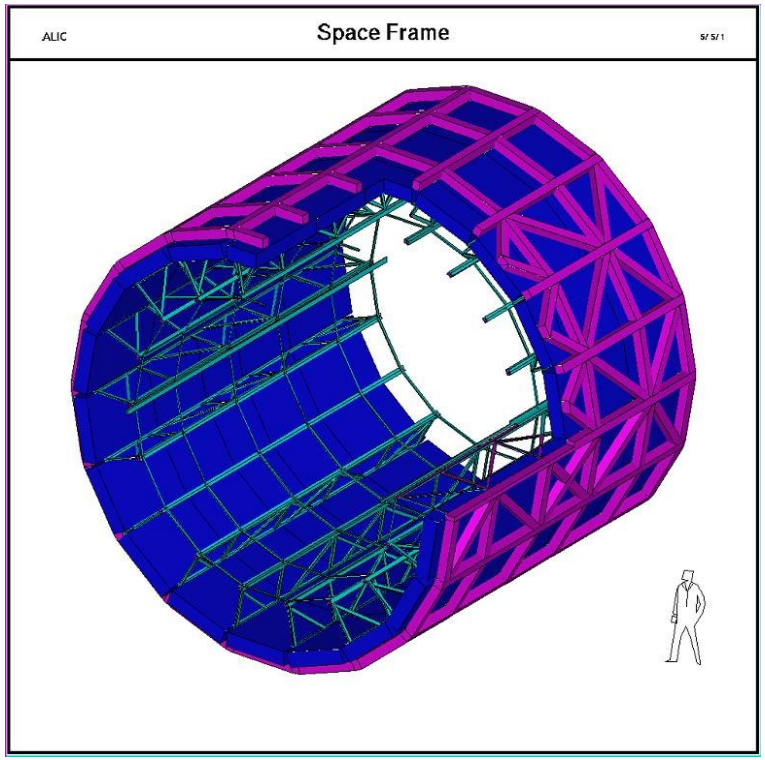

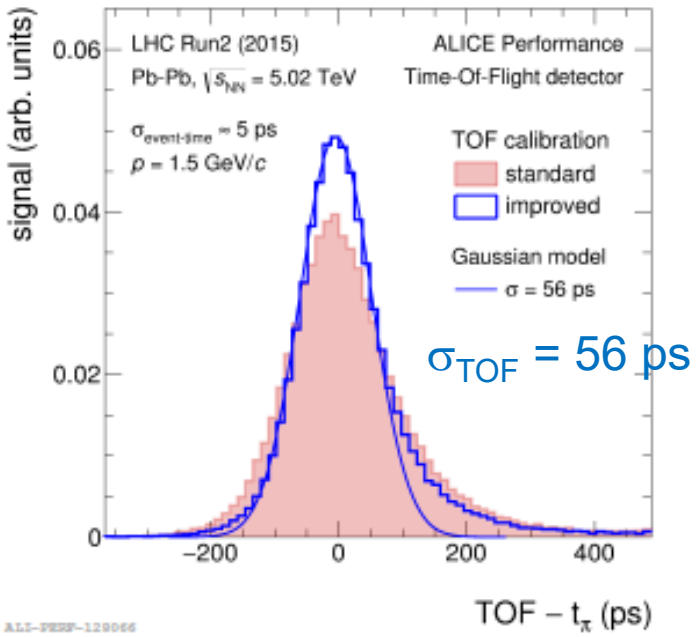

σ_{TOF} = 56 ps

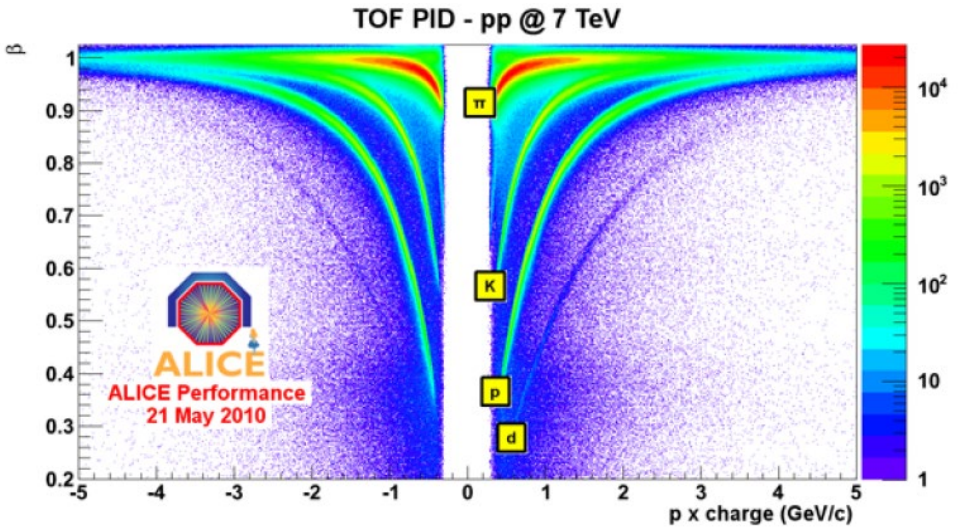

Measurement of Cherenkov angle:

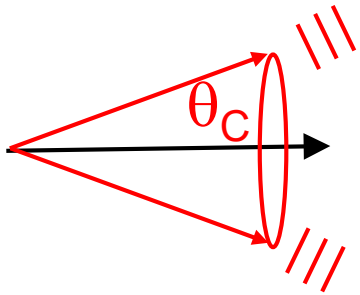

$$\cos\theta_C = \frac{1}{\beta n}$$

With $$\beta = \frac{1}{\sqrt{\left(\frac{mc}{p}\right)^2 + 1}}$$

one finds for the mass:

$$m = \frac{p}{c}\sqrt{n^2\cos^2(\Theta_C) - 1}$$

Average measurement error $\left\langle \sigma_{\theta_C} \right\rangle$

(several effects contribute)

Separation in sigmas:

$$n_{\sigma_{\Theta_C}} = \frac{\Theta_{C,A} - \Theta_{C,B}}{\langle \sigma_{\Theta_C} \rangle}$$

One can derive the mass separation for $\beta \approx 1 > \beta_{Thresh}$ as function of the angular resolution to measure θ_C

$$n_{\sigma_{\Theta_C}} \approx \frac{c^2}{2p^2\langle \sigma_{\Theta_C} \rangle \sqrt{n^2 - 1}} |m_B^2 - m_A^2|$$

(see for example C. Amsler et al. (PDG), Phys. Let. B667 (2008) 1.)

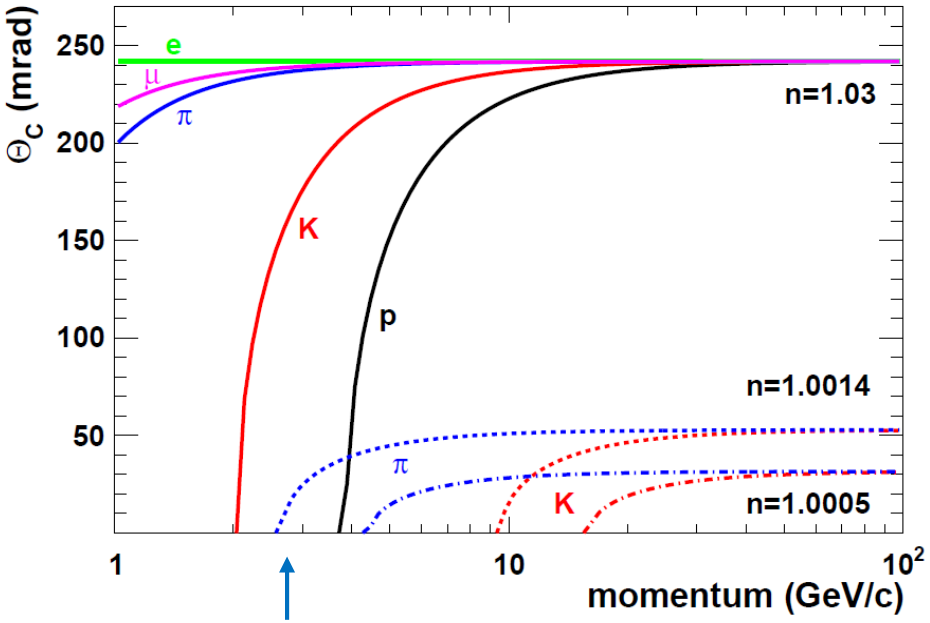

Threshold given by $\beta > 1/n$

Example: LHCb Ring Imaging Cherenkow Detector

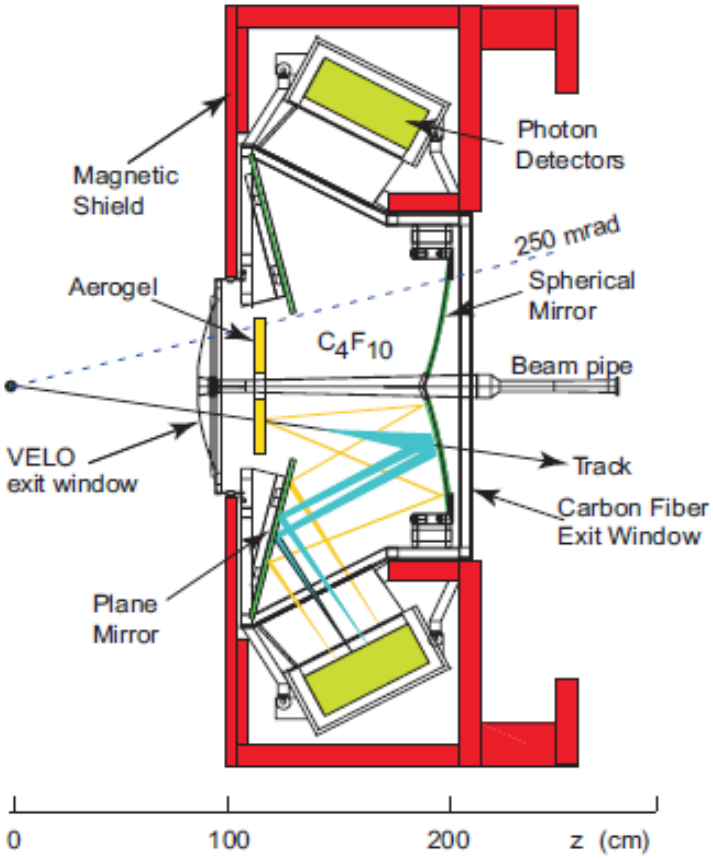

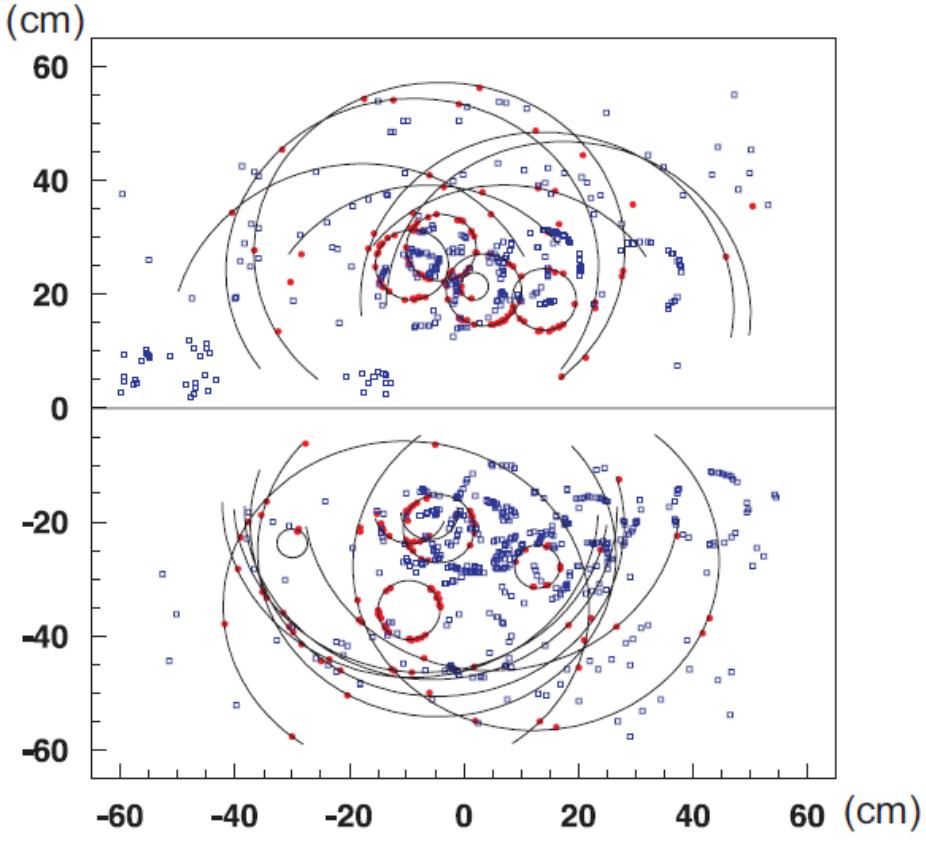

Refractive index: Aerogel n=1.037 → large rings

C_4F_{10} n=1.0015 → small rings

Comparison: Different PID systems

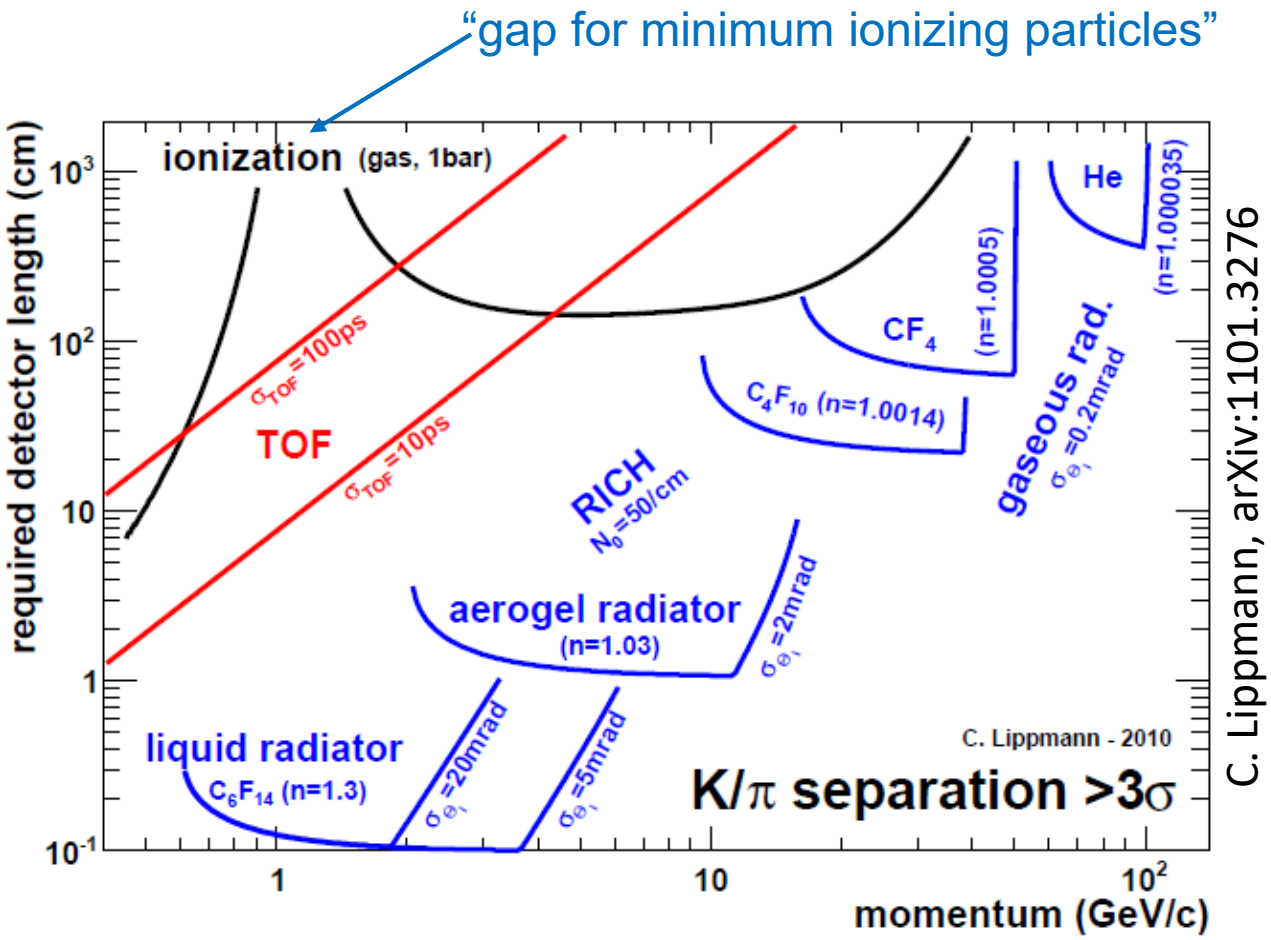

5. Detector systems

(only one example)

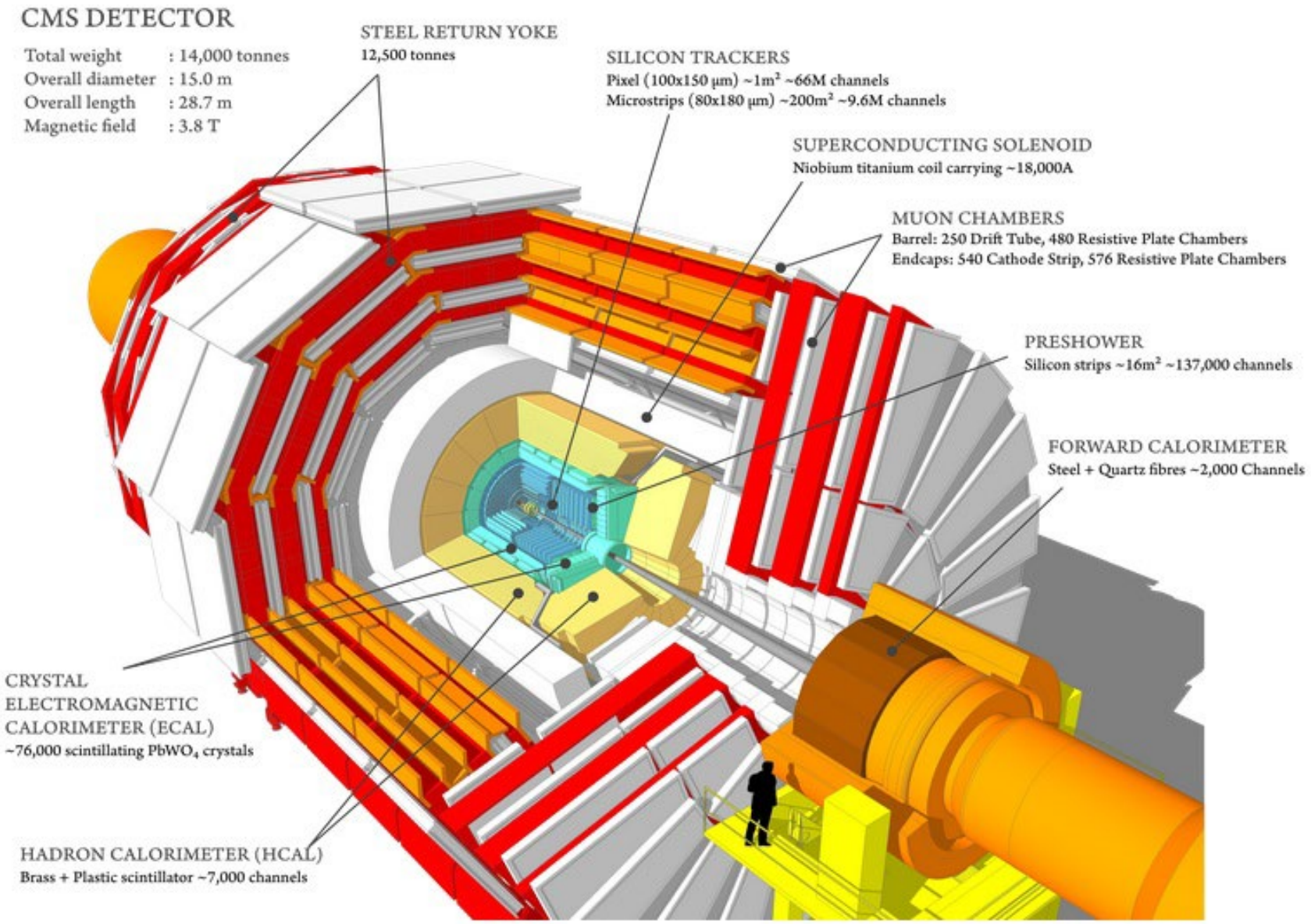

Particle signatures in the CMS detector:

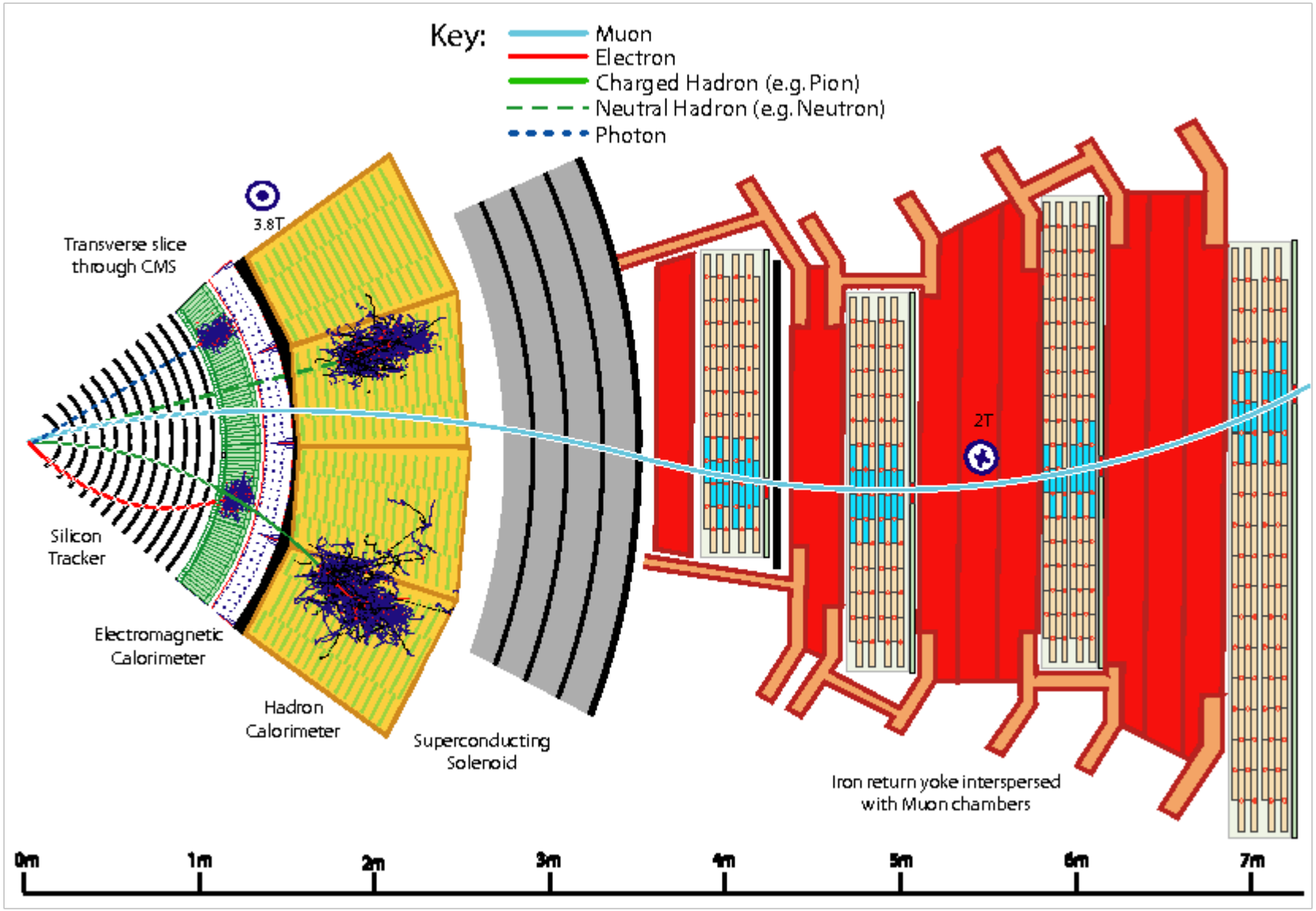

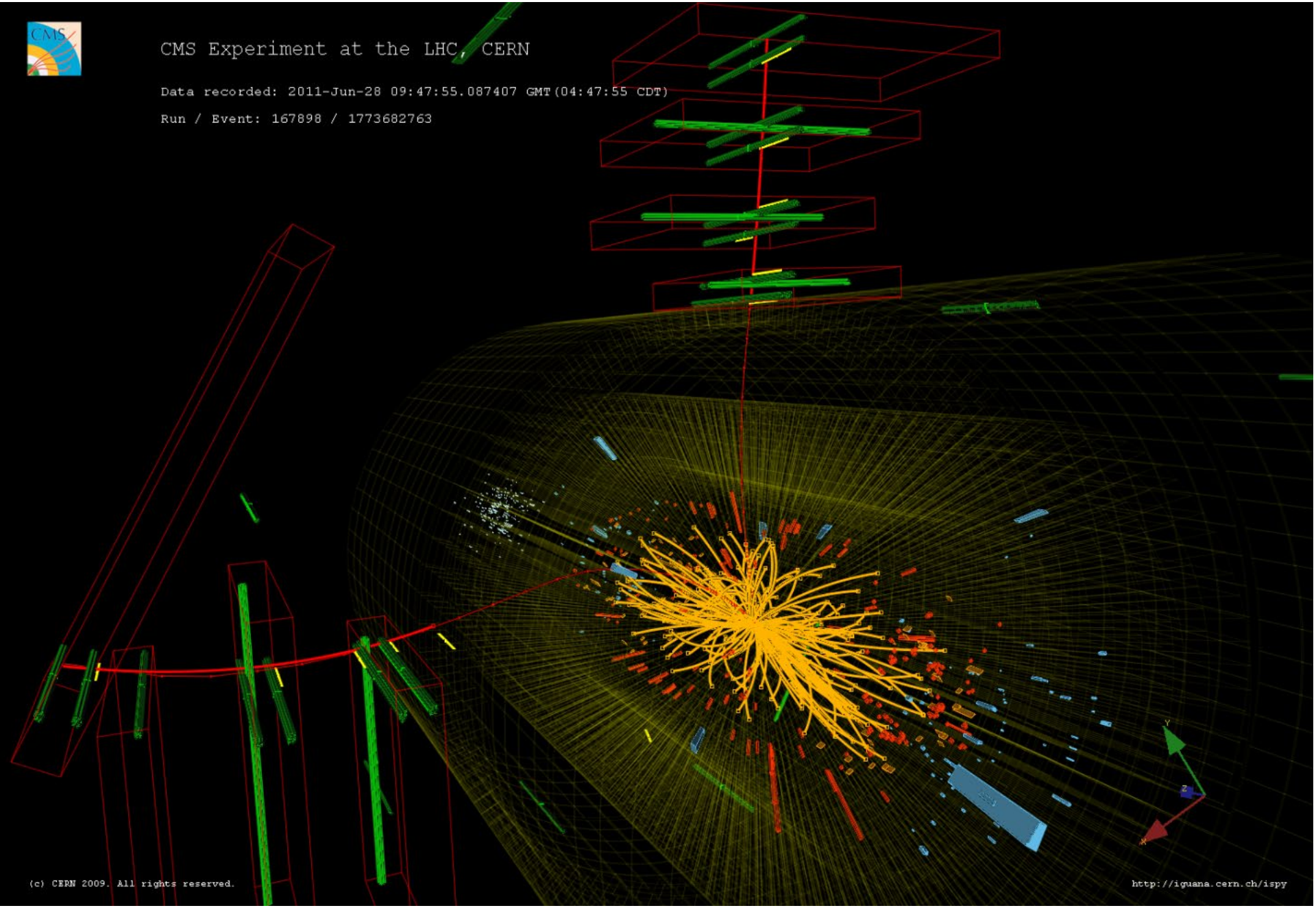
CMS Experiment at the LHC, CERN
Data recorded: 2011-Jun-28 09:47:55.087407 GMT(04:47:55 CDT)
Run / Event: 167898 / 1773682763
(c) CERN 2009. All rights reserved.
http://iguana.cern.ch/ispy

LHCb Detector

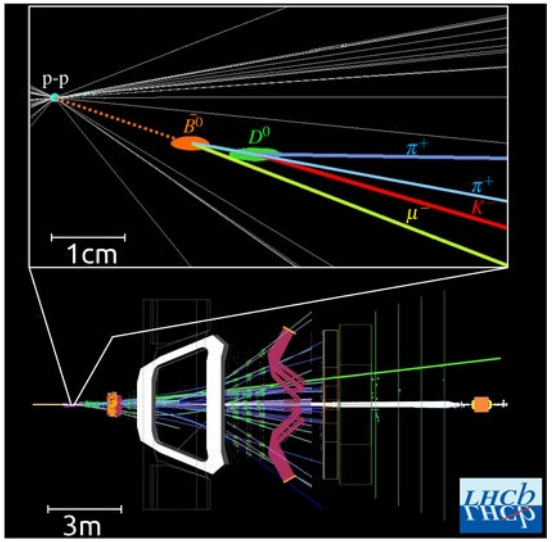

Pinpointing Bs
Millimetres from where collisions occur, short-lived B hadrons decay into other particles. A new 'vertex locator' will measure this point with greater precision.

Tracking particles
'Trackers' trace particle paths. Two new detectors will better separate nearly identical paths and cut out the noise that mimics real tracks.

Charged hadron (such as a proton or pion)
Electron
Muon

Muon detector
Detector
Tracker
Detector
Beamline: particle bunches collide here
Magnet: bends the path of charged particles
Calorimeters: measure a particle's energy

Electronics
Renovated electronics mean that LHCb can now use software to scan through 40 million events per second. Previously, a coarser hardware filter first triaged these to identify one million to be scanned.

Identifying particles
Other detectors measure the velocity of charged particles; combining this information with a particle's path reveals its identity. Upgraded detectors are more sensitive to velocity and can cope with higher data rates.